UNIVERSIDADE DO ESTADO DE SANTA CATARINA
CENTRO DE EDUCAÇÃO SUPERIOR DA FOZ DO ITAJAÍ
ENGENHARIA DE PETRÓLEO

LEONARDO HENRIQUE PAZ

OTIMIZAÇÃO DE CONTROLADOR DE TANQUE SEPARADOR BIFÁSICO COM ALGORITMO EVOLUCIONÁRIO

BALNEÁRIO CAMBORIÚ

2017

LEONARDO HENRIQUE PAZ

OTIMIZAÇÃO DE CONTROLADOR DE TANQUE SEPARADOR BIFÁSICO COM ALGORITMO EVOLUCIONÁRIO

Este trabalho tem como objetivo a conclusão do curso superior em Engenharia de Petróleo ofertado pela Fundação Universidade do Estado de Santa Catarina a fim do recebimento do diploma e do título de Engenheiro de Petróleo.
Orientador: Aníbal Alexandre Campos Bonilla

BALNEÁRIO CAMBORIÚ
2017

LEONARDO HENRIQUE PAZ

OTIMIZAÇÃO DE CONTROLADOR DE TANQUE SEPARADOR BIFÁSICO COM ALGORITMO EVOLUCIONÁRIO

Este trabalho tem como objetivo a conclusão do curso superior em Engenharia de Petróleo ofertado pela Fundação Universidade do Estado de Santa Catarina a fim do recebimento do diploma e do título de Engenheiro de Petróleo.

Banca Examinadora:

Orientador:

_____

Aníbal Alexandre Campos Bonilla
UDESC

Membros:

_____

Débora Cristina Brandt
UDESC

_____

Marina Enricone Stasiak
UDESC

_____

Ellen Kindermann
Engenheira de Petróleo

BALNEÁRIO CAMBORIÚ
2017

ACKNOWLEDGEMENTS

RESUMO

Esse trabalho apresenta a otimização de dois controladores de um tanque separador bifásico cujo principal objetivo é amortecer os efeitos de um fluxo intermitente de gás e líquido. O modelo do tanque separador é linearizado e dois controladores Proporcional-Integral-Derivativo (PID) são implementados para o controle do nível do líquido e da pressão do gás. A otimização dos parâmetros é feita com um Algorítimo Genético. Esse algorítimo minimiza a amplitude da fração de abertura das válvulas de líquido e gás, e também os desvios do nível, da pressão e do fluxo de saída, mantendo os parâmetros PID dentro de valores estipulados. É possível ver nos resultados que o método converge em poucas iterações, mantendo as frações de abertura das válvulas, nível de líquido e pressão do gás em pequenas amplitudes. Essas baixas variações garantem maior vida útil ao tanque e às válvulas, resultando em menor necessidade de reparos e economia de recursos.

Palavras-chave: Teoria de Controle, Otimização de Parâmetros, Algoritmo Genético, Simulação Numérica, Controle PID

ABSTRACT

This work presents two controllers optimization for a biphasic separator which main objective is to damp intermittent liquid and gas flow effects. The separator tank model is linearized and two Proportional-Integral-Derivative (PID) controllers are implemented to control its liquid level and gas pressure. This parameters optimization is done using a Genetic Algorithm function. This algorithm minimizes valves opening fraction amplitude for liquid and gas and deviations for liquid level, gas pressure and outlet liquid flow while keeping the PID parameters bounded. Results show that the method converges to an optimal value in few iterations, keeping valves opening fractions, liquid level and gas pressure within small range values. This low variation assures longer life span for the tank and valves which results in less maintenance and resources saving.

Keywords: Control theory, Parameter optimization, Genetic algorithm, Numerical simulation, PID control.

LIST OF FIGURES

LIST OF TABLES

LIST OF SYMBOLS

q, Q or F	Volumetric flow rate
V	Volume
h or H	Fluid level
A	Cross-sectional area
R_v	Valve's resistence to flow
ρ	Fluid density
m or M	Mass
t	Time
u	Heat
α	Thermal diffusivity coefficient or derivative filter
θ	Angle
$:=$	Definition
g	Gravity constant
L	Length
$\mathscr{L}$	Laplace Transform Operator
s	Laplace variable
f'	First derivative of f
f''	Second derivative of f
$f^{(n)}$	n-th derivative of f
$S(t)$	Step function
τ	Time constant
$\mathscr{L}^{-1}$	Inverse Laplace Transform
x_i	Concentration of component i
w	Mass flow rate
N_F	Degree of freedom

N_V	Number of process variables
N_E	Number of independent equations
$G_i(s)$ or $H(s)$	Transfer function
ψ'	Deviation of ψ (generic variable)
$\bar{\psi}$	Value of ψ in steady state
$Y(s)$	Generic Laplace output variable
$X_i(s)$ or $U(s)$	Generic Laplace input variable
K_i	Gain
K_m	Sensor constant
$e(t)$ or $E(s)$	Setpoint error
K_c or K_p	Proportional gain
$p(t)$	Generic input
τ_I	Integral Time
I_i	Proportional gain divided by integral time
τ_D	Derivative time
D_i	Proportional gain multiplied by derivative time
z_i	Zero of a transfer function
p_i	Pole of a transfer function
∇	Gradient
λ	Lagrange multiplier
c_v	Valve's flow coefficient
$f(x_v)$	Valve's dimensionless flow characteristic
x_v	Liquid or gas valve opening fraction, $(v = L, G)$
ΔP	Pressure drop throughout the valve
ρ_f	Relative fluid density
T	Temperature

P_1	Upstream gas valve pressure
R	Valve's rangeability
C	Tank's length
D	Tank's diameter
L_{in}	Inlet volumetric liquid flow
L_{out}	Outlet volumetric liquid flow
MM	Molar mass
R_G	Universal gas constant
G_{in}	Inlet volumetric gas flow
G_{out}	Outlet volumetric gas flow
P_2	Upstream liquid valve pressure
C_{VL}	Liquid valve flow constant
C_{VG}	Gas valve flow constant
$\rho_{H_2O,15.5^oC}$	Water density

LIST OF ABBREVIATIONS AND ACRONYMS

GA	Genetic Algorithm
ANN	Artificial Neural Network
PID	Proportional-Integral-Derivative
ODE	Ordinary Differential Equation
PDE	Partial Differential Equation
SS	Steady State
sp	Setpoint
PI	Proportional-Integral
PD	Proportional-Derivative
SISO	Single-Input Single-Output
MIMO	Multiple-Input Multiple-Output
GOR	Gas-Oil Ratio
PSO	Particle Swarm Optimization

CONTENTS

1 INTRODUCTION

1.1 MOTIVATION

Slug flow is an unwanted behavior during petroleum extraction and separation. This intermittent liquid and gas flow results in low quality separation and flooding in separator tanks, liquid flowing through the gas valve, wearing and corrosion in equipment and tubing, flaring, and eventually plant shutdown due to high liquid level inside the separator tank (GODHAVN et al., 2004).

Bai and Bai (2016) state that slug flow may induce problems to operation and project processes, including kinectic forces in equipment, oscillatory pressure, instability in the control system and inadequate separation. Swindell (2011) also relates intermittent flow to tubing oscillation, even calling it a "hidden threat" since this is hardly ever perceived in oil platforms topside. Up to 21% of platforms topside tubing fail can be related to vibrational problems (SWINDELL, 2011).

Godhavn et al. (2004) present reasons why controlling slug flow is important. Less plant shutdowns translates to major economic enhancement besides improved oil quality after separation and increased life span of equipment. Several optimization tools are available to solve engineering problems like this, and metaheuristic algorithms have been extensively implemented.

Genetic Algorithms (GA) are metaheuristic methods that have been widely explored in solving engineering problems and have proved to be efficient in finding good solutions. Romero and Carter (2001) characterized oil reservoirs using a special GA resulting in a robust solution that could be used in automatic reservoir characterization algorithms. Ahmadi et al. (2013) developed an effective and robust oil flow predicting method by evolving an Artificial Neural Network (ANN). Güyagüler et al. (2002) implemented a GA with other solving methods to a waterflooding project which decreased the number of iterations needed to solve the problem and prevented issues related to stochastic simulations. Camargo et al. (2010) predicted reservoir oil flow using GA and obtained results equivalent to commercial softwares. Ghaedi et al. (2014) optimized multistage separation pressures in separator tanks with a GA, resulting in a larger oil recovery factor in the end of the process.

1.2 OBJECTIVE

1.2.1 Main Objective

The main objetive of this work is to optimize a biphasic separator tank liquid level and gas pressure control using a genetic algorithm method to find optimal PID parameter values.

1.2.2 Specific Objectives

- Literature review of mathematical, physical and computational tools;

- Literature review of genetic algorithm;

- Develop a biphasic separator tank model and PID control strategy;

- Simulate and optimize PID parameters.

1.3 STRUCTURE

In Section 2 several tools ranging from mathematical to computational that helps solving the optimization problem are reviewed. In Section 3 the model and its parameters are presented. Results from the optimization are shown in Section 4 and an in-depth discussion is made in Section 5, where suggestions for future works are also presented.

2 LITERATURE REVIEW

2.1 MATHEMATICAL TOOLS

This section contains a brief explanation of Differential Equations, Laplace Transforms and Taylor Series.

2.1.1 Differential Equations

Several natural phenomena occur as functions of the rate that variables change (BOYCE; DIPRIMA, 2004). Mathematically, the behavior of these systems can be modeled as relationships of derivatives, called **Differential Equations**. Algebraic Equations result in values; Differential Equations result in functions. For instance, consider the tank system of Figure 1.

Figure 1 – Tank System
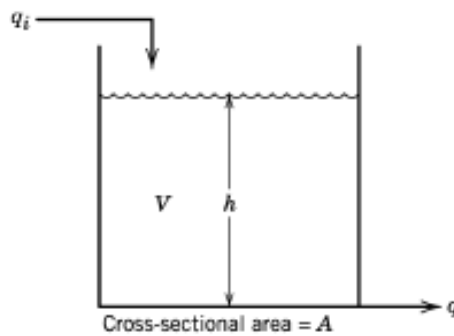
Source: SEBORG et al. (2011).

This system contains an inlet volumetric flow q_i, an outlet volumetric flow q, a fluid volume V which level is h, and a cross-sectional area A. Suppose there is a valve that controls q that behaves as

$$q = \frac{1}{R_v}h, \tag{2.1}$$

where R_v is the flow resistence constant. Assuming the fluid is incompressible with constant density ρ, the tank behavior can be modeled by a conservation of mass equation:

$$\frac{dm}{dt} = \dot{m}_i - \dot{m}$$

$$\frac{d}{dt}(\rho V) = \rho q_i - \rho q$$

$$\frac{d}{dt}(\rho A h) = \rho q_i - \rho q$$

$$\rho A \frac{dh}{dt} = \rho q_i - \rho q$$

$$A\frac{dh}{dt} = q_i - q. \tag{2.2}$$

Substituting Equation 2.1 in Equation 2.2 results in

$$A\frac{dh}{dt} = q_i - \frac{1}{R_v}h. \tag{2.3}$$

Equation 2.3 is a differential equation since ir relates dh/dt and h. Solving this equation will result in a function that describes the behavior of h as a function of time. Section 2.1.2 will explore this topic further.

Another example is the heat flow equation,

$$\alpha\frac{\partial^2 u(x,t)}{\partial x^2} = \frac{\partial u(x,t)}{\partial t}. \tag{2.4}$$

This equation also relates the derivative of u in respect to x axis and time t. Solving this equation results in the behavior of heat flow as a function of time and space.

Boyce and DiPrima (2004) present some differential equations classifications:

Ordinary and Partial Differential Equations. Ordinary Differential Equations (ODE) solutions are functions of a single independent variable; Partial Differential Equations (PDE) solutions are functions of several independent variables. Therefore, Equation 2.3 is an ODE and Equation 2.4 is a PDE.

Differential Equation System. When more than one differential equation is required to solve a specific problem, it is a system of differential equations. The number of equations in this system must be equal to the number of unknown functions.

Order. A differential equation order is equal to the higher order derivative in the equation. Therefore, Equation 2.3 is a first order ODE whilst Equation 2.4 is a second order PDE.

Linearity. A linear differential equation can be written as

$$a_0(t)y^{(n)} + a_1(t)y^{(n-1)} + \cdots + a_n(t)y = g(t). \tag{2.5}$$

It is possible to conclude then that both Equations 2.3 and 2.4 are linear. An example of a non-linear differential equation occurs when deriving a pendulum system:

$$\frac{d^2\theta}{dt^2} + \frac{g}{L}\text{sen}(\theta) = 0. \tag{2.6}$$

Since it is significantly more difficult to deal with non-linear differential equation, it is a common practice to linearize them. This topic will be further studied in Sections 2.1.3 and 2.2.3.

Solution. A differential equation solution is a function that satisfies the conditions of a differential equation.

2.1.2 Laplace Transform

There are several methods available to solve differencial equations. This work focuses in the Laplace Transform. Being $f(t)$ a function defined to $t \geq 0$ and continuous by parts, the Laplace Transform is

$$\mathscr{L}\{f(t)\} = F(s) := \int_0^\infty e^{-st} f(t) dt, \tag{2.7}$$

when this integral converges. Examples 1 to 4 in Annex A refer to solving Laplace Transforms. Some known Laplace Transforms are presented in Table B.1.

Laplace Transform Properties

Two main properties can be used to solve differential equations: the fact that it is a linear operation and an injective function.

i) Its linearity is inherited by the integral definition, because

$$\int [af(x) + bg(x)] dx = a \int f(x) dx + b \int g(x) dx. \tag{2.8}$$

where $a, b \in \mathfrak{R}$. Since the Laplace Transform is defined as an integral, it is possible be show that

$$\mathscr{L}\{af(x) + bg(x)\} = a\mathscr{L}\{f(x)\} + b\mathscr{L}\{g(x)\}. \tag{2.9}$$

ii) Being an injective function means that an inverse function can be defined. In this case, an Inverse Laplace Transform exists in such a way that

$$\mathscr{L}^{-1}\{F(s)\} = f(t). \tag{2.10}$$

It is possible to see now that the Laplace Transform is a powerful tool to solve differential equations. Table B.1 transforms a differential equation in an algebraic equation, allowing us to solve for $F(s)$. Then, the inverse transform can be applied to find $f(t)$.

2.1.3 Taylor Series

Let $f(x)$ be a continuous function in all of its domain with also continuous derivatives. This function can be expressed as an infinite polynomial series (STEWART, 2007),

$$\begin{aligned} f(x) &= \sum_{n=0}^\infty c_n (x-a)^n \\ &= c_0 + c_1(x-a) + c_2(x-a)^2 + \cdots. \end{aligned} \tag{2.11}$$

Coefficients c_n are calculated by evaluating the previous expressions and its derivatives in $x = a$.

$$f(a) = c_0. \tag{2.12}$$

$$f'(a) = c_1. \tag{2.13}$$

$$f''(a) = 2c_2; \tag{2.14}$$

$$\begin{aligned} f'''(a) &= 2 \times 3c_3 \\ &= 3!c_3, \end{aligned} \tag{2.15}$$

and so on. The n-th coefficient is defined as

$$c_n = \frac{f^{(n)}(a)}{n!}. \tag{2.16}$$

Equating Equations 2.11 and 2.16 wields

$$f(x) = \sum_{n=0}^{\infty} \frac{f^{(n)}(a)}{n!}(x-a)^n. \tag{2.17}$$

Equation 2.17 is defined as the Taylor Series in a and it is used to approximate functions by a summation of polynomials with more or less precision. The more terms evaluated before truncating the series, the more precise the approximation is. In Example 5 from Annex A, the function sen (θ) is approximated by a Taylor Series.

This is a powerful tool to approximate non-linear differential equations by linear differential equations. For instance, the pendulum system of Equation 2.6 could be linearized by approximating the function sen (θ) by θ, which is Equation A.13 truncated in the first term. This topic will be further studied in Section 2.2.3.

2.2 PHYSICAL TOOLS

In this section, the steps to model a physical system are explained followed by an explanation on transfer functions model and linearization of non-linear models.

2.2.1 Modeling Physical Systems

There are four main reasons to model a physical system (SEBORG et al., 2011):

1) *It improves understanding of the process*. Dynamic models allow investigating the transient process behavior without actually disturbing the process;

2) *Can be used to train plant operating personnel*;

3) *Control strategy development.* It allows evaluating different control strategies and identifying controlled and manipulated variables;

4) *Process operating conditions optimization.* It allows recalculating optimum operating conditions periodically in order to maximize profit or minimize costs.

Next, a systematic approach is presented in order to model a physical process:

1) state modeling objectives and determine required levels of model detail and accuracy;

2) draw a schematic diagram of the process and label all process variables;

3) list all assumptions involved, the model should not be overly complicated;

4) determine whether or not spatial variation is relevant. If so, PDEs will be required;

5) write appropriate conservation equations;

6) introduce equilibrium relations and other algebraic equations (thermodynamics, transport phenomena, chemical kinectis, etc.);

7) perform a degrees of freedom analysis;

8) simplify the model;

9) classify inputs as disturbance variables or as manipulated variables.

Conservation laws have a major role in modeling physical processes since they describe the behavior of energy and matter. Some important examples are the Conservation of Mass, the Conservation of Component and the Conservation of Energy.

Conservation of Mass

$$\{\text{accumulated mass}\} = \{\text{mass in}\} - \{\text{mass out}\} \tag{2.18}$$

Conservation of Component *i*

$$\{\text{accumulated } i \text{ component}\} = \{i \text{ component in}\} - \{i \text{ component out}\} \tag{2.19}$$

Conservation of Energy

Second law of Thermodynamics:

$$\{\text{accumulated energy}\} = \{\text{energy in}\} - \{\text{energy out}\} \tag{2.20}$$

Example 1

Consider the following tirred-tank from Figure 2. There are two inlet flows of a single component where x_1 and x_2 are the concentration of each flow and w_1 and w_2 are the mass flow rates. Both streams are blended resulting in a volume V. There is also an exit flow w with concentration x, both unkown. A constant density ρ will be considered. Since it is desired to know two variables behavior, a system of two differential equations will be needed.

Supose the blending occurs instantly and homogeneously so the concentration of the whole fluid is x. In order to model this system, the conservation of mass (Equation 2.18) and component (Equation 2.19) are written below:

$$\rho \frac{dV}{dt} = w_1 + w_2 - w, \tag{2.21}$$

Figure 2 – Stirred-Tank
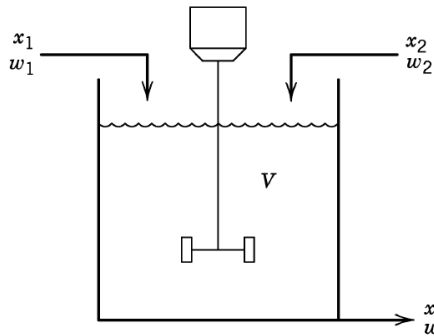
Source: SEBORG et al. (2011).

$$\rho \frac{d(Vx)}{dt} = w_1 x_1 + w_2 x_2 - wx. \tag{2.22}$$

Solving this system requires separating V and x. Thus, the chain rule is applyed,

$$\rho x \frac{dV}{dt} + \rho V \frac{dx}{dt} = w_1 x_1 + w_2 x_2 - wx. \tag{2.23}$$

Knowing $\rho dV/dt$ from Equation 2.21 allows further simplification:

$$x(w_1 + w_2 - w) + \rho V \frac{dx}{dt} = w_1 x_1 + w_2 x_2 - wx \tag{2.24}$$

Rearranging the system yields

$$\frac{dV}{dt} = \frac{1}{\rho}(w_1 + w_2 - w) \tag{2.25}$$

$$\frac{dx}{dt} = \frac{w_1}{V\rho}(x_1 - x) + \frac{w_2}{V\rho}(x_2 - x) \tag{2.26}$$

That is, the stirred-tank blending system was modeled using the laws of conservation. Solving this system of differential equations will result in the functions that describe the behavior of V and x over time.

After deriving the physical process model, analyzing the degree of freedom is a necessary step since the system of differential equations must be solvable. The number of unknown variables must be equal to the number of differential equations (see Section 2.1.1). The degree of freedom N_F is defined as

$$N_F = N_V - N_E, \tag{2.27}$$

where N_V is the number of process variables and N_E is the number of independent equations in the model. Three scenarios emerge from this (SEBORG et al., 2011):

1) $N_F = 0$: The process model is exactly specified and has a solution;

2) $N_F > 0$: The process model is underspecified ans has an infinite number of solutions;

3) $N_F > 0$: The process model is overspecified and has no solution.

The previous example has two equations and two unknown functions, therefore it is exactly specified an has a solution.

2.2.2 Transfer Functions

Transfer Functions have an important role in the analysis of control systems. These functions describe the dynamic relationship between two process variables in Laplace Domain, that can only be applyied to linear ODE systems (SEBORG et al., 2011).

Let $x(t)$ be an input process variable which correspondent in Laplace domain is $X(s)$, and $y(t)$ an output variable with a correspondent $Y(s)$. The transfer fuction between these two variables is defined as

$$G(s) := \frac{Y(s)}{X(s)}. \tag{2.28}$$

This function is calculated by applying the Lapace Transform in the dynamic model of the process and solving for $Y(s)/X(s)$. Using transfer functions model requires initial conditions to be zero, which can be achieved by introducing deviation variables.

A deviation variable is defined as the deviation from equilibrium,

$$x' := x - \bar{x}, \tag{2.29}$$

where x' is the deviation variable, $\bar{x}$ is the value at equilibrium and x is the actual value. Since a process is usually analyzed after a disturbance occurs, deviation variables will always be zero in the initial condition.

Take the tank from Section 2.1.1 again as example, modeled by Equation 2.3,

$$A\frac{dh}{dt} = q_i - \frac{1}{R_v}h.$$

The input variable is q_i and the output is h, and their correspondent in Laplace domain are $Q_i(s)$ and $H(s)$. During steady state,

$$A\frac{d\bar{h}}{dt} = \bar{q}_i - \frac{1}{R_v}\bar{h}, \tag{2.30}$$

even though $d\bar{h}/dt$ is zero. Subtracting Equation 2.30 from 2.3,

$$A\frac{d(h-\bar{h})}{dt} = (q_i - \bar{q}_i) - \frac{1}{R_v}(h-\bar{h}). \tag{2.31}$$

Introducing deviation variables,

$$\begin{cases} h' = h - \bar{h} \\ q_i' = q_i - \bar{q}_i, \end{cases}$$

Equation 2.31 becomes

$$A\frac{dh'}{dt} = q_i' - \frac{1}{R_v}h'. \tag{2.32}$$

Now initial conditions are zero and transfer function model can be used.

Applying Laplace Transform in both sides,

$$AsH'(s) = Q'_i(s) - \frac{1}{R_v}H'(s), \tag{2.33}$$

$$H'(s) = \frac{R_v Q'_i(s)}{(R_v A)s + 1}. \tag{2.34}$$

Finally, rearranging it so it takes the form of Equation 2.28, the transfer function is found,

$$G(s) = \frac{H'(s)}{Q'_i(s)} \\ = \frac{R_v}{(R_v A)s + 1}. \tag{2.35}$$

When there are more than one input variables, several transfer functions coexist and can be written as

$$\begin{cases} G_1(s) := \frac{Y(s)}{X_1(s)} \\ G_2(s) := \frac{Y(s)}{X_2(s)} \\ \vdots \\ G_n(s) := \frac{Y(s)}{X_n(s)}; \end{cases}$$

$$Y(s) = G_1(s)X_1(s) + G_2(s)X_2(s) + \cdots + G_n(s)X_n(s). \tag{2.36}$$

Tranfer function model has noteworthy advantages such as (SEBORG et al., 2011):

1) Transfer Functions are additive;

2) input variables that are not relevant may be considered constant when studying a specific deviation;

3) allows studying one input variable at a time.

2.2.3 Linearization

As stated before, transfer function method can only be applied to linear models. In Section 2.1.1 though it was presented that even simple phenomena such as a pendulum may result non-linear models. It is a common practice then to linearize non-linear models using the Taylor Series Expansion seen in Section 2.1.3.

Take a non-linear dynamic model such as

$$\frac{dy}{dt} = f(y, u), \tag{2.37}$$

where y is the output variable and u is the input variable. Linearization is done by expanding $f(y, u)$ in Taylor Series at $(\bar{y}, \bar{u})$ and truncating it in the first term:

$$f(y, u) \approx f(\bar{y}, \bar{u}) + \frac{\partial f}{\partial y}\bigg|_{(\bar{y}, \bar{u})} (y - \bar{y}) + \frac{\partial f}{\partial u}\bigg|_{(\bar{y}, \bar{u})} (u - \bar{u}). \tag{2.38}$$

When working with deviation variables, $f(\bar{y}, \bar{u}) = 0$ (SEBORG et al., 2011). The terms inside the brackets are the definition of deviation variables presented in Equation 2.29. Since $d\bar{y}/dt = 0$, Equation 2.37 becomes

$$\frac{dy'}{dt} = \left.\frac{\partial f}{\partial y}\right|_{SS} y' + \left.\frac{\partial f}{\partial u}\right|_{SS} u', \tag{2.39}$$

where the subindex *SS* indicates evaluation at steady state and therefore these values are constants.

Example 2

The model derived in Example 1 is described by Equations 2.25 and 2.26,

$$\rho \frac{dV}{dt} = (w_1 + w_2 - w)$$

$$\rho V \frac{dx}{dt} = w_1(x_1 - x) + w_2(x_2 - x),$$

assuming constant V (therefore $w = w_1 + w_2$) and $x_2 = 1$.

Equation 2.26 is non-linear since x multiplies both variables w_1 and w_2. This equation has to be linearized in order to apply the transfer function model. From Equation 2.39, Equation 2.26 is approximated by

$$\rho V \frac{dx'}{dt} = \left(\frac{\partial f}{\partial x}\right)_{SS}(x - \bar{x}) + \left(\frac{\partial f}{\partial x_1}\right)_{SS}(x_1 - \bar{x}_1) + \left(\frac{\partial f}{\partial w_1}\right)_{SS}(w_1 - \bar{w}_1) + \\ \left(\frac{\partial f}{\partial w_2}\right)_{SS}(w_2 - \bar{w}_2). \tag{2.40}$$

Evaluating the derivatives:

$$\begin{cases} \left(\frac{\partial f}{\partial x}\right)_{SS} = -\bar{w}_1 - \bar{w}_2 \\ \left(\frac{\partial f}{\partial x_1}\right)_{SS} = \bar{w}_1 \\ \left(\frac{\partial f}{\partial w_1}\right)_{SS} = \bar{x}_1 - \bar{x} \\ \left(\frac{\partial f}{\partial w_2}\right)_{SS} = 1 - \bar{x} \end{cases} \tag{2.41}$$

$$\therefore \rho V \frac{dx'}{dt} = -\bar{w}x' + \bar{w}_1 x' + (\bar{x}_1 - \bar{x})w_1' + (1 - \bar{x})w_2' \tag{2.42}$$

The model is now linear at equilibrium and transfer function model can be used. Applying Laplace Transform yields

$$\rho V s X'(s) = -\bar{w}X'(s) + \bar{w}_1 X_1'(s) + (\bar{x}_w - \bar{x})W_1'(s) + (1 - \bar{x})W_2'(s)$$

$$\left(\frac{V\rho}{\bar{w}}s + 1\right)X'(s) = \frac{\bar{w}_1}{\bar{w}}X_1'(s) + \frac{\bar{x}_1 - \bar{x}}{\bar{w}}W_1'(s) + \frac{1 - \bar{x}}{\bar{w}}W_2'(s)$$

$$\begin{cases} \tau := \frac{V\rho}{\bar{w}} \\ K_1 := \frac{\bar{w}_1}{\bar{w}} \\ K_2 := \frac{1 - \bar{x}}{\bar{w}} \\ K_3 := \frac{\bar{x}_1 - \bar{x}}{\bar{w}} \end{cases}$$

$$X'(s) = \frac{K_1}{\tau s + 1} X_1'(s) + \frac{K_2}{\tau s + 1} W_2'(s) + \frac{K_3}{\tau s + 1} W_1'(s). \tag{2.43}$$

From Equation 2.36,

$$\begin{cases} G_1(s) := \frac{X'(s)}{X_1'(s)} = \frac{K_1}{\tau s+1} \\ G_2(s) := \frac{X'(s)}{W_2'(s)} = \frac{K_2}{\tau s+1} \\ G_3(s) := \frac{X'(s)}{W_1'(s)} = \frac{K_3}{\tau s+1} \end{cases} \tag{2.44}$$

It's important to keep in mind that the linearization process is an approximation around a specific point (equilibrium). The further away from this point, the less representative the approximation will be.

2.3   CONTROL SYSTEMS

In this section, dynamic systems are represented as Block Diagrams, which makes easier to understand the relationship between input and output variables. Then classic Closed Loops Control Strategies are introduced followed by a Dynamic Response Characteristics of Processes analysis. Finally, a brief explanation of Multiple-Input Multiple-Output Systems will take place.

2.3.1   Block Diagram

A Block Diagram is a physical process graphical representation that allows treating complex systems with simple operations such as sums and multiplications (NUNES et al., 2010). An example is shown in Figure 3.

Figure 3 – Block Diagram
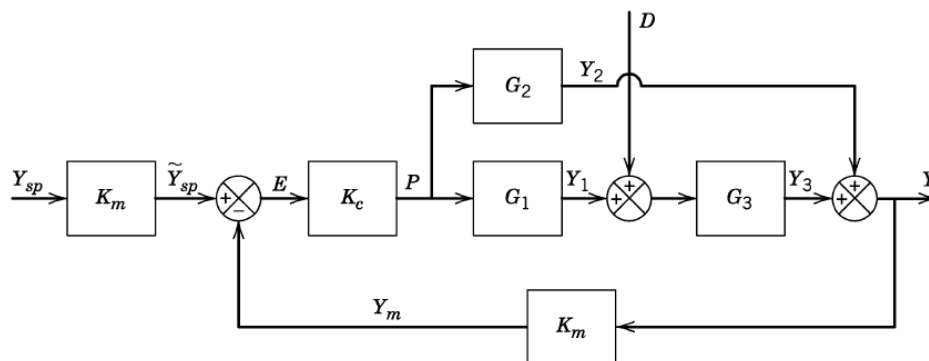
Source: SEBORG et al. (2011).

The block diagram structures are (NUNES et al., 2010):

1) **Variables**. Shown over the lines that represent information flow direction;

2) **Blocks**. Contain transfer functions between the block input and output variable. For instance, the block in the far left of Figure 3 can be interpreted as

$$\frac{\tilde{Y}_{sp}}{Y_{sp}} = K_m; \tag{2.45}$$

These blocks represent equipment, plants, machines, sensors, etc, that interact with the variables.

3) **Summation Point**. Where variables summation or subtraction happens (Figure 4).

Figure 4 – Sumation Point
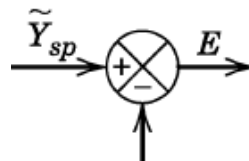
Source: adapted from SEBORG et al. (2011).

4) **Derivation Point**. Point where a variable information splits in more than one direction (Figure 5).

Figure 5 – Derivation Point
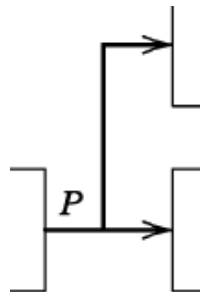
Source: adapted from SEBORG et al. (2011).

The system presented in Figure 3 starts with a setpoint value of Y_{sp}, in the left hand side, which is the controlled variable Y desired value; the system output variable is the actual value of Y, in the right hand side.

A pattern often present in a block diagram is a feedback loop, shown in Figure 6.

It can be demonstrated that the feedback is equivalent to the following expression (NUNES et al., 2010):

$$\frac{Y(s)}{U(s)} = \frac{G(s)}{1 + G(s)H(s)}. \tag{2.46}$$

It is then possible to see that Figure 3 contains a feedback loop where the loop transfer function is K_m, often called sensor constant.

Figure 6 – Feedback loop

Source: NUNES et al. (2010).

2.3.2 Control Strategies

A feedback loop compares the actual output variable value to the desired setpoint value. If they are not equal, it is desired that some action is taken so the actual value will meet the setpoint value. This action is reffered as Control Strategy. Seborg et al. (2011) introduces three basic control models: Proportional Control, Integral Control and Derivative Control.

2.3.2.1 Proportional Control (P)

The setpoint error is defined as

$$e(t) = y_{sp}(t) - y_m(t), \qquad (2.47)$$

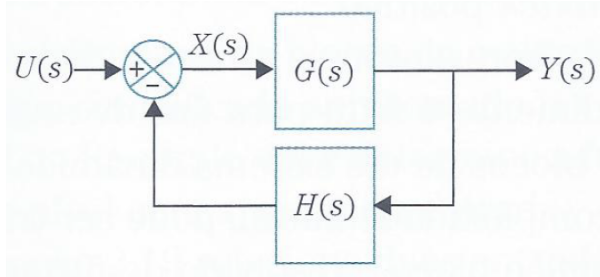where $y_{sp}(t)$ is the setpoint value and $y_m(t)$ is the measured value. Proportional Control adds the error value multiplied by a constant K_c to the setpoint, thus increasing or decreasing the system input proportionally to the error

$$p(t) = \bar{p} + K_c e(t), \qquad (2.48)$$

where $p(t)$ is the updated input, $\bar{p}$ is original input and K_c is the Proportional Gain. Proportional Control acts proportionally to the error absolute value.

Introducing deviation variables to Equation 2.48 so it is possible to write it in transfer function fashion results in

$$p'(t) = K_c e(t), \qquad (2.49)$$

since $e(t)$ is already defined as a deviation variable.

Applying Laplace transform yields

$$\frac{P'(s)}{E(s)} = K_c. \qquad (2.50)$$

Back to Figure 3, it's now possible to identify a proportional controler in the block diagram, as shown in the crop of Figure 7.

An inherent disadvantage in this control strategy is that it results in a steady state offset from the desired setpoint (Figure 8). This topic is explored further in SEBORG et al. (2011).

Figure 7 – Proportional Controler in Figure 3
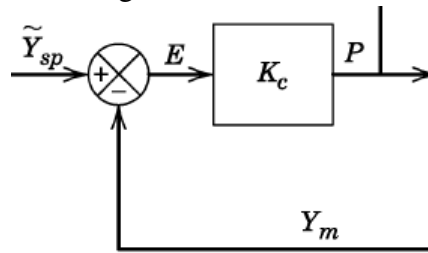
Source: adapted from SEBORG et al. (2011).

Figure 8 – Proportional Controller Offset
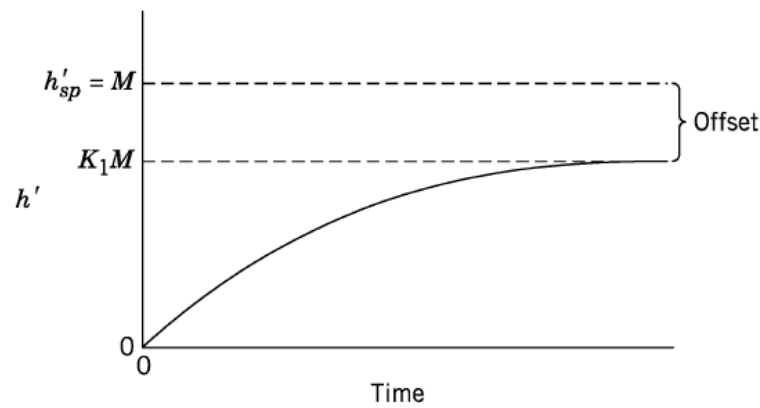
Source: SEBORG et al. (2011).

2.3.2.2 Integral Control (I)

Integral action is written as

$$p(t) = \bar{p} + \frac{1}{\tau_I} \int_0^t e(t)dt, \tag{2.51}$$

where τ_I is defined as Integral Time. The integral controller takes action over the integral of the error over time. This takes rid of the offset seen in the proportional control, but this controller may take longer to act. Therefore, Integral Control is rarely ever implemented by itself. It is common though to use proportional and integral control together, defined as PI controller (Proportional-Integral):

$$p(t) = \bar{p} + K_c \left(e(t) + \frac{1}{\tau_I} \int_0^t e(t)dt \right), \tag{2.52}$$

which transfer function model is

$$\begin{aligned} \frac{P'(s)}{E(s)} &= K_c \left(1 + \frac{1}{\tau_I s} \right) \\ &= K_c \left(\frac{\tau_I s + 1}{\tau_I s} \right). \end{aligned} \tag{2.53}$$

When an step error $e(t)$ takes place, PI controller takes an instant action in $t = 0$ due to the proportional action, followed by a ramp due to the integral action. This behavior is illustrated in Figure 9.

Figure 9 – PI controller behavior when a step error takes place.
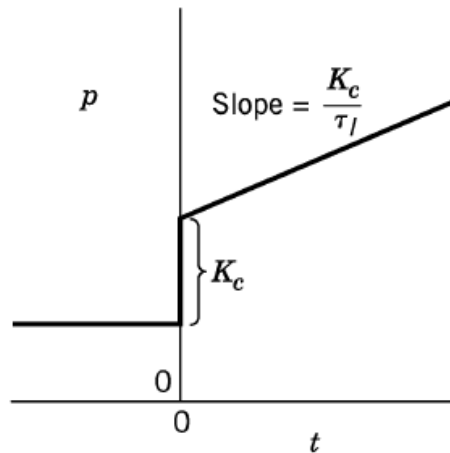
Source: SEBORG et al. (2011).

2.3.2.3 Derivative Control (D)

Derivative control action is

$$p(t) = \bar{p} + \tau_D \frac{de(t)}{dt}, \tag{2.54}$$

where τ_D is the derivative time. This controller antecipates the error behavior by reading its derivative. It can be seen in the previous equation though that it only takes action when the derivative is not 0, even if the error itself is not 0. Therefore, derivative control never takes place by itself and is always implemented together with a P or PI controller. A PD controller's transfer function is as follows:

$$\frac{P'(s)}{E(s)} = K_c(1 + \tau_D s). \tag{2.55}$$

When a system shows noisy readings, the derivative control tends to desestabilize since it will try to read a constantly changing derivative. In practice, an ideal PD controller is not feasible, so an approximation is done to Equation 2.55,

$$\frac{P'(s)}{E(s)} = K_c \left(1 + \frac{\tau_D s}{\alpha \tau_D s + 1} \right), \tag{2.56}$$

where the α constant ranges between 0.05 and 0.2. The equation denominator acts as a derivative filter that reduces the sensibility to noisy readings (SEBORG et al., 2011).

2.3.2.4 PID Controller

The PID Controller is the combination of all the previous controllers. It is a largely spread control strategy and up to 97% of all industrial processes uses some type of PID controller (SEBORG et al., 2011; NUNES et al., 2010). Among these types there are the Parallel and Series PID Controller.

Parallel PID Controller

A parallel PID controller is shown in Figure 10 and its transfer function without a derivative filter is

$$\frac{P'(s)}{E(s)} = K_c \left[1 + \frac{1}{\tau_I s} + \tau_D s \right].$$ (2.57)

Figure 10 – Parallel PID Controller.
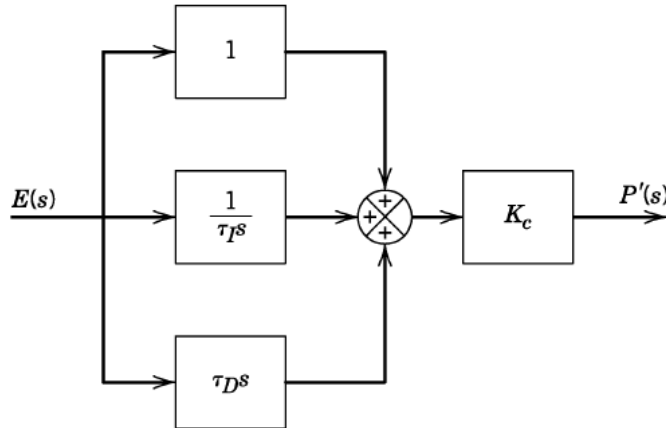
Source: SEBORG et al. (2011).

Series PID Controller

A series PID controller is shown in Figure 11 and its transfer function with a derivative filter is

$$\frac{P'(s)}{E(s)} = K_c \left(\frac{\tau_I s + 1}{\tau_I} \right) \left(\frac{\tau_D s + 1}{\alpha \tau_D s + 1} \right).$$ (2.58)

Figure 11 – Series PID Controller
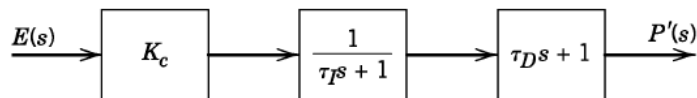
Source: SEBORG et al. (2011).

2.3.3 Dynamic Response Characteristics of Processes

Given a transfer function as shown in Equation 2.59, the denominator of this equation influences the behavior of the process (SEBORG et al., 2011).

$$\frac{Y(s)}{X(s)} := G(s) = \frac{\sum_{i=0}^{m} b_i s^i}{\sum_{i=0}^{n} a_i s^i}$$

$$= \frac{b_m s^m + b_{m-1} s^{m-1} + \cdots + b_0}{a_n s^n + a_{n-1} s^{n-1} + \cdots + a_0}.$$ (2.59)

where $a_i, b_i \in \Re$, $i = 0, 1, ..., m, ..., n$.

The previous equation can be written in terms of numerator and denominator roots, defined as *zeros* (z_i) and *poles* (p_i), respectively:

$$\frac{Y(s)}{X(s)} = \frac{b_m}{a_n} \frac{(s - z_1)(s - z_2) \cdots (s - z_m)}{(s - p_1)(s - p_2) \cdots (s - p_n)} \tag{2.60}$$

For a physical system to be feasible, there must be more poles than zeros in its transfer function, that is, $m \leq n$ (SEBORG et al., 2011). This is the reason why the ideal PD controller is not feasible in Section 2.3.2.3.

Assuming no reocurring poles and an input step variable $X(s) = 1/s$, Equation 2.60 can be expanded in partial fractions:

$$Y(s) = \frac{A_0}{s} + \frac{A_1}{s - p_1} + \frac{A_2}{s - p_2} + \cdots + \frac{A_n}{s - p_n}. \tag{2.61}$$

Applying the inverse Laplace transform, it is possible to see that the behavior of $y(t)$ is

$$y(t) = A_0 + A_1 e^{p_1 t} + A_2 e^{p_2 t} + \cdots + A_n e^{p_n t}. \tag{2.62}$$

For any $p_i > 0$, Equation 2.62 will increase indefinitely, thus becoming unstable. On the contrary, if all p_i are negative, the system will converge (SEBORG et al., 2011). Poles and zeroes can be plotted in a complex plane and a qualitative analysis can be done. In Figure 12, three arbitrary poles were plotted on a complex plane, each one represented by an x.

Figure 12 – Poles in a complex plane.
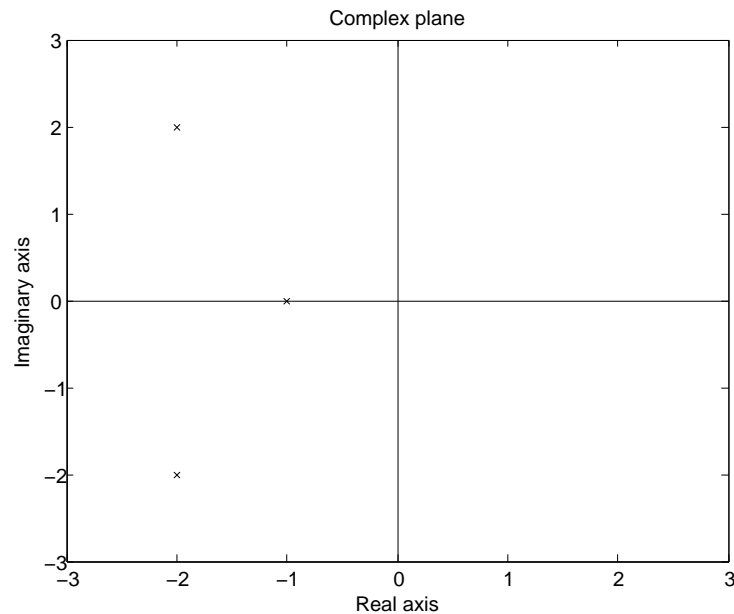
Source: author, 2017.

Poles on the left-half plane (negative real part) are stable. The more negative the real part, the faster the pole will act. This is due to $e^{p_i t}$ reducing its absolute value quickly if p_i is a large negative number.

Imaginary numbers, as represented by the conjugate pair in Figure 12, will induce oscillations in the system because they result in trigonometric functions in Equation 2.62 (SEBORG et al., 2011).

2.3.3.1 Routh Stability Criterion

As stated before, a dynamic system can only be stable if all of its poles are located on the left-half complex plane. In 1905, Routh developed a method to verify if a polynomial has any root with a positive real part. This method is called the Routh Stability Criterion. This method can only be used in polynomials in s (SEBORG et al., 2011).

Take the roots of the Equation 2.59 denominator,

$$a_n s^n + a_{n-1} s^{n-1} + \cdots + a_1 s + a_0 = 0. \tag{2.63}$$

It is assumed that a_n is positive. This identity is called the transfer function Characteristic Equation. A necessary but not sufficient condition to stability is that all coefficients must be positives and non-zero. If this is not true, at least one root will have a positive real part. If true, the Routh Matrix can be written as shown in Figure 13.

Figure 13 – Routh Matrix.

Row				
1	a_n	a_{n-2}	a_{n-4}	$\cdots$
2	a_{n-1}	a_{n-3}	a_{n-5}	$\cdots$
3	b_1	b_2	b_3	$\cdots$
4	c_1	c_2	$\cdots$	
$\vdots$	$\vdots$			
$n+1$	z_1			

Source: SEBORG et al. (2011).

Routh Matrix contains $n+1$ rows and coefficients from Equation 2.63 are written in the first two rows in the order shown in Figure 13. Coefficients b_i, c_i, ..., z_i are calculated by

$$b_1 = \frac{a_{n-1} a_{n-2} - a_n a_{n-3}}{a_{n-1}} \tag{2.64}$$

$$b_2 = \frac{a_{n-1} a_{n-4} - a_n a_{n-5}}{a_{n-1}} \tag{2.65}$$

$$\vdots$$

$$c_1 = \frac{b_1 a_{n-3} - a_{n-1} b_2}{b_1} \tag{2.66}$$

$$c_2 = \frac{b_1 a_{n-5} - a_{n-1} b_3}{b_1} \tag{2.67}$$

$$\vdots$$

which numerator is but the negative of the determinant of a 2×2 matrix while the denominator is the first term of the previous row.

In the end, the matrix will be roughly triangular with a single term in the last row. Routh Stability Criterion states: *A necessary and sufficient condition for all roots of the characteristic equation in Equation 2.63 to have negative real parts is that all of the elements in the left column of the Routh array are positive* (SEBORG et al., 2011).

Example 3

Take a feedback loop with a proportional controller K_c that is described by the following transfer function:

$$Y(s) = \frac{K_c(s+1)}{10s^3 + 17s^2 + 8s + 1 + K_c} \cdot \frac{1}{s}. \tag{2.68}$$

To find a stable value of K_c, the Routh method is applied. The system characteristic equation is

$$10s^3 + 17s^2 + 8s + (1 + K_c) = 0 \tag{2.69}$$

in which case $a_0 = 1 + K_c$ and therefore $K_c > -1$ since all coefficients must be positives right away. Arranging Routh Matrix:

$$
\begin{array}{ll}
10 & 8 \\
17 & (1 + K_c) \\
b_1 &
\end{array}
$$

Coefficient b_1 is calculated by Equation 2.64:

$$
\begin{aligned}
b_1 &= \frac{136 - 10(1 + K_c)}{10} \\
&= 12.6 - K_c,
\end{aligned} \tag{2.70}
$$

and there are no more coefficients because the characteristic equation is a third degree polynomial.

All coefficients in the first column must be positives, in which case

$$
\begin{aligned}
b_1 &> 0, \\
\therefore K_c &< 12.6.
\end{aligned} \tag{2.71}
$$

Therefore, $-1 < K_c < 12.6$ in order for this system be stable.

2.3.4 Multiple-Input, Multiple-Output (MIMO) Systems

Up until now, only Single-Input Single-Outputs (SISO) or Single-Loop Systems were presented. In practice, several processes involve more then one input and output. These complex systems are labeled Multiple-Input Multiple-Output (MIMO) systems or Multi-Loop Systems.

Figure 14 – *Multi-loop* system of a biphasic separator.
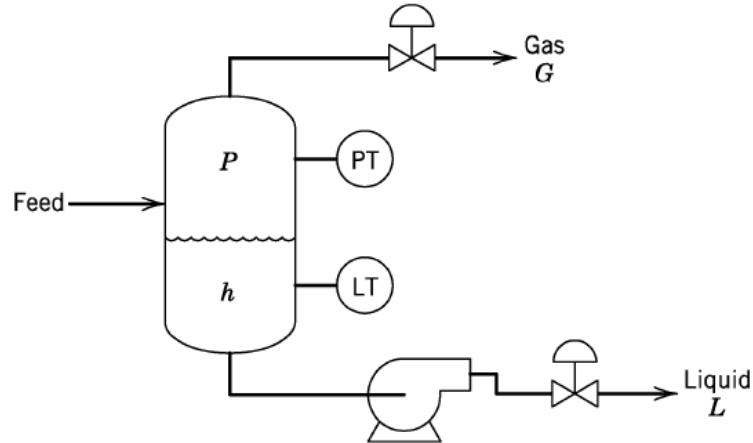
Source: SEBORG et al. (2011).

Biphasic separators are classic examples of MIMO, as shown in Figure 14.

The disturbance variable is its feed, which is a liquid and gas flow mixture. Controlled variables are liquid level and gas pressure, and the manipulated variables are the liquid and gas valves opening fractions.

MIMO systems are inherently more complex than SISO systems. In general, a change in any of the input variables (setpoints) will affect all output variables. Taking a 2 inputs 2 outputs example (2×2), a system of four transfer functions will arise when the dynamic model is derived, shown in Equation 2.72 and Figure 15.

$$\begin{cases} \frac{Y_1(s)}{U_1(s)} = G_{p11}(s); \\ \frac{Y_1(s)}{U_2(s)} = G_{p12}(s); \\ \frac{Y_2(s)}{U_1(s)} = G_{p21}(s); \\ \frac{Y_2(s)}{U_2(s)} = G_{p22}(s). \end{cases} \tag{2.72}$$

The system presented in Figure 15 hides a third loop involving all four transfer functions, shown in Figure 16.

MIMO systems stability is similar to SISO systems. A 2×2 MIMO system can be represented by

$$Y_1 = \Gamma_{11} Y_{sp1} + \Gamma_{12} Y_{sp2} \tag{2.73}$$

$$Y_2 = \Gamma_{21} Y_{sp1} + \Gamma_{22} Y_{sp2}, \tag{2.74}$$

where the transfer functions are

$$\Gamma_{11} = \frac{G_{c1} G_{p11} + G_{c1} G_{c2} (G_{p11} G_{p22} - G_{p12} G_{p21})}{\Delta(s)} \tag{2.75}$$

$$\Gamma_{12} = \frac{G_{c2} G_{p12}}{\Delta(s)} \tag{2.76}$$

Figure 15 – 2 × 2 MIMO system.
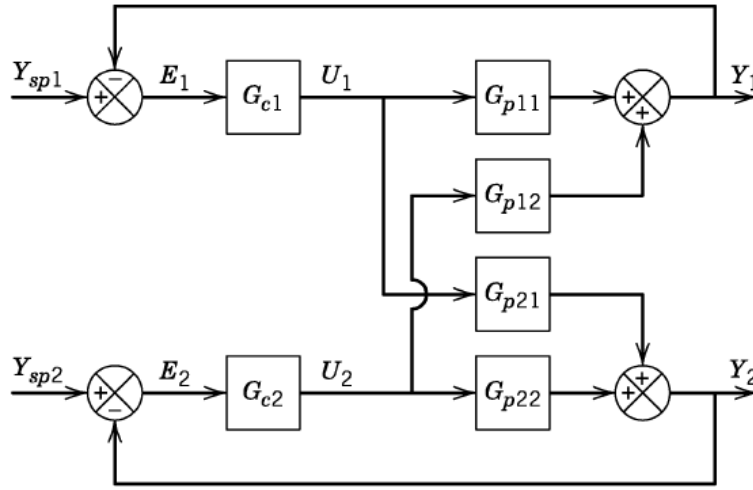
Source: SEBORG et al. (2011).

Figure 16 – Hidden loop.
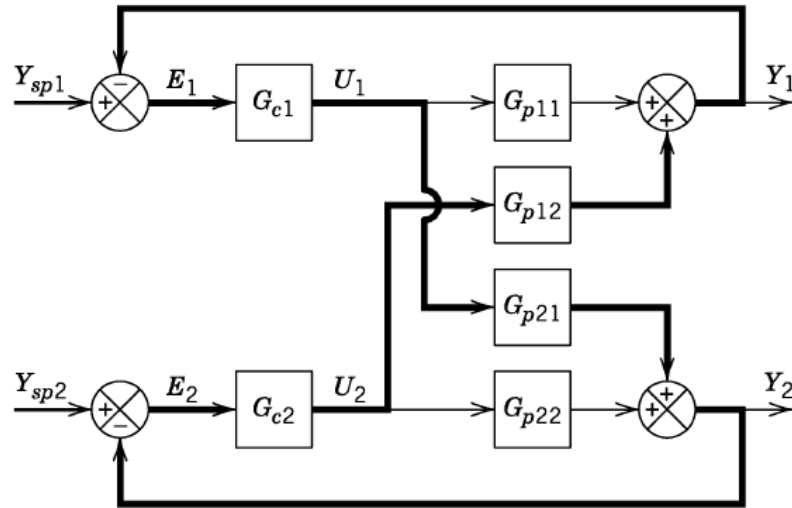
Source: SEBORG et al. (2011).

$$\Gamma_{21} = \frac{G_{c1}G_{p21}}{\Delta(s)} \tag{2.77}$$

$$\Gamma_{22} = \frac{G_{c2}G_{p22} + G_{c1}G_{c2}(G_{p11}G_{p22} - G_{p12}G_{p21})}{\Delta(s)} \tag{2.78}$$

and the characteristic polinomial is

$$\Delta(s) = (1 + G_{c1}G_{p11})(1 + G_{c2}G_{p22}) - G_{c1}G_{c2}G_{p12}G_{p21}. \tag{2.79}$$

Stability region is found applying Routh criterion to $\Delta(s) = 0$, that is, the system's characteristic equation.

2.4   COMPUTATIONAL TOOLS

2.5   MATLAB

This work uses MATLAB Optimization Toolbox (2009) to solve the optimization problem. MATLAB (2009) is a mathematical simulation and data analysis software. It contains two environments: a workspace and an editor (Figure 17).

Figure 17 – MATLAB's (2009) environments. Left: workspace, Right: editor.

Fonte: Printscreen from MATLAB (2009).

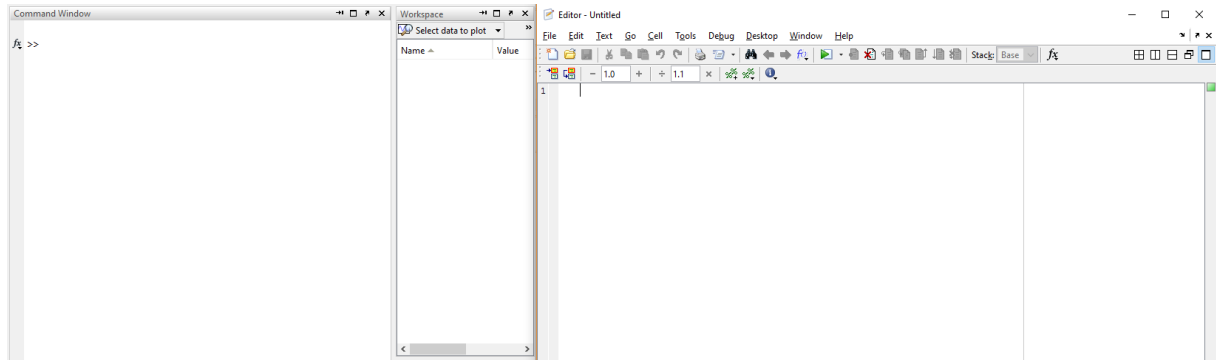Besides MATLAB (2009), this work uses SIMULINK, which is its dynamic systems simulator package.

2.6   SIMULINK

SIMULINK accompanies MATLAB (2009) as a dynamic system simulator package with a friendly UI, allowing to build block diagrams, simulate and analyze data (NUNES et al., 2010). Typing *simulink* in MATLAB's workspace opens the Library Browser window (Figure 18) with several block options to create a block diagram. This library contains a Sources section, Sinks, Continuous, Math Operations, and so on.

To start a block diagram, the user must click on the New Model button (white sheet) on the upper left corner of the library window. Nunes et al. (2010) provide a step-by-step guide to create and simulate a diagram:

1) drag the desired blocks to the simulation window;

2) connect the blocks the same way as the model (click the first block and then Control-click the next one);

3) configure all blocks (double click);

4) configure the simulation (Simulation → Configure Parameters, on the upper bar);

5) simulate;

Figure 18 – SIMULINK Library Browser.
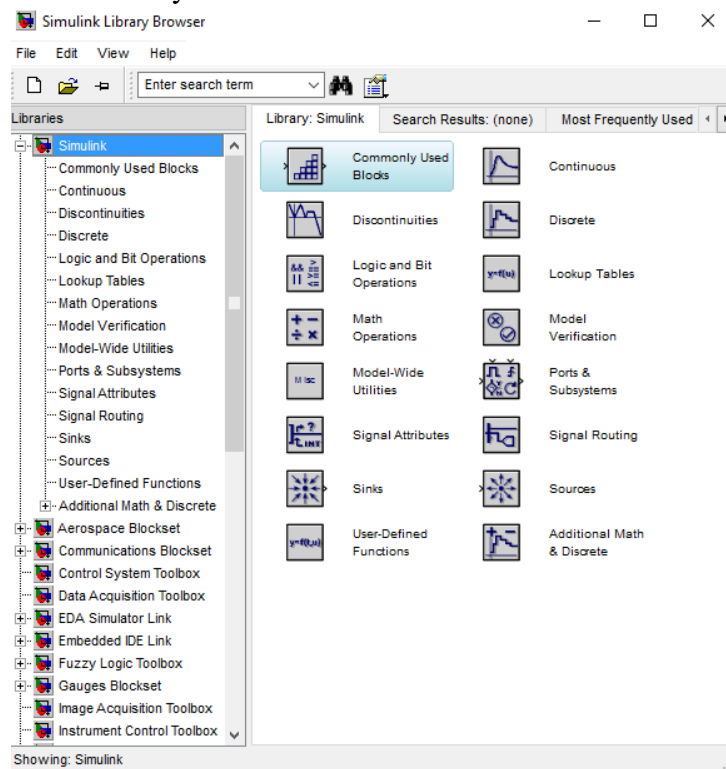
Source: *Printscreen* from SIMULINK.

6) analyze the outputs with the Sinks library.

Example

The block diagram from Figure 3 in Section 2.3.1 can be built in SIMULINK, setting the transfer functions and gains arbitrarily, as shown in Figure 19.

Figure 19 – Diagram from Figure 3 in SIMULINK.

Source: Printscreen SIMULINK.

Setpoint is chosen to be 10, and the disturbance D was set as a step function with magnitude 2 and initial time equals 3 seconds. Simulation time is set to 10 seconds. After simulating, double clicking the Scope block allows visualizing the model response, shown in Figure 20.

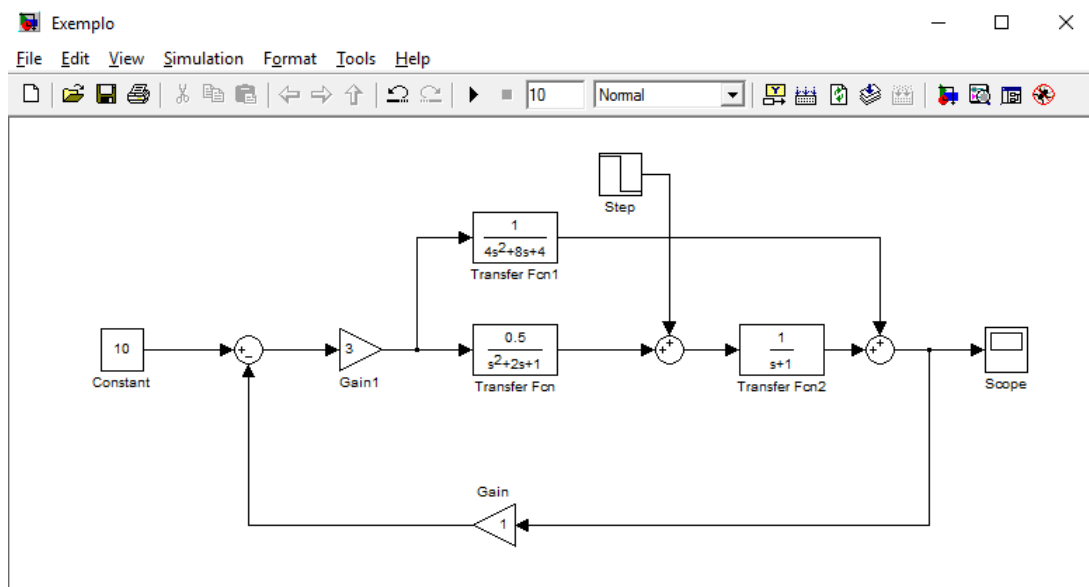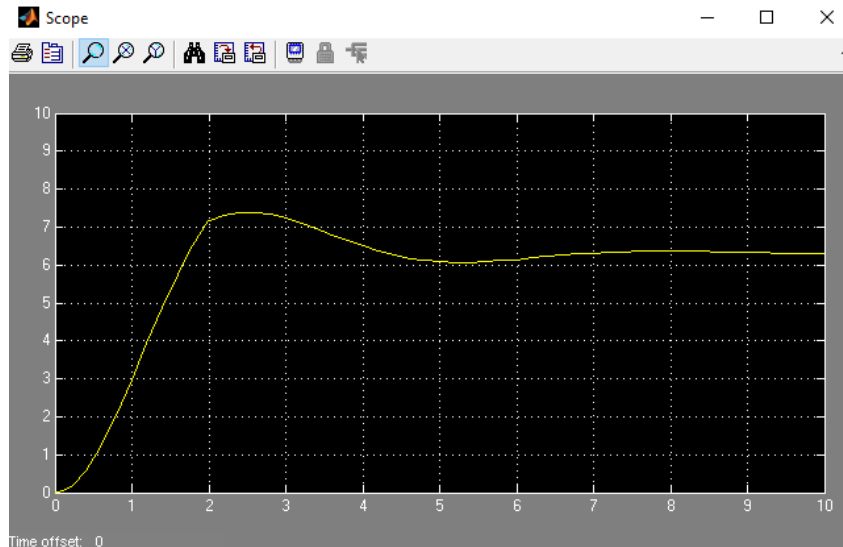Figure 20 – Example response.

Source: Printscreen from SIMULINK.

2.7   PRIMARY PROCESSING

This section briefly explains natural petroleum occurance and how this influences the processing plant project. Next, the separator tank is explained and slug flows will be studied.

2.7.1   Petroleum Occurrence

Petroleum is generated by decomposition of large quantities of organic material under intense heat and pressure. This material is then accumulated in "source rocks" and underground pressure and capillary distribution cause it to migrate until it finds an impermeable rock layer. The organic matter is then stored in a porous and permeable rock called "reservoir rock" (SILVA et al., 2007).

Frequently, underground fluids are arranged as shown in Figure 21 due to gravity segregation and phase imiscibillity. Therefore, not only petroleum is produced but also gas, water and solids (SILVA et al., 2007). None of these phases is isolated from each other. Gas is present in oil as bubbles, water vapor is carried by gas or oil-water emulsion is formed. Even free water contains solids, dissolved gas and carried oil (SILVA et al., 2007). When this mixture arrives at the platform, separation is required.

Different phases are used for different ends and they may introduce hazards to the general process. Oil is destined to refinaries, water is recycled to secondary recovery or discarded, gas

Figure 21 – Underground fluids.
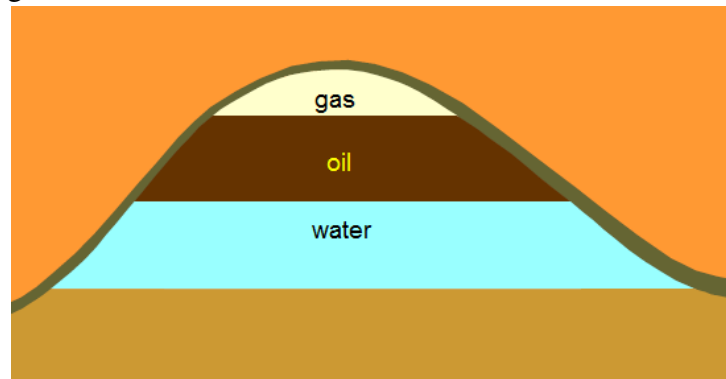
Source: adapted from SILVA et al. (2007).

may be used in turbines (NUNES et al., 2010). Some hazards include little to no economic value in water, that also carries salts (chlorides, sodium carbonates and sulfates, calcium, barium, magensium, etc), resulting in corrosion and inorganic inlay in equipment and lines (SILVA et al., 2007). Also, water presence may induce gas hydrates formation, which are crystalline structures that occur when light fractions of oil gas meet low temperatures and high pressures. Therefore, water and gas coexistence may block flow lines partially or completely (SILVA et al., 2007). Aiming at separating this mixture, a series of equipment defined Primary Processing Plant performs several levels of liquid-liquid and gas-liquid separation.

2.7.2 Processing Plant

Primary processing happens both in onshore and offshore structures and its main goals are to (SILVA et al., 2007):

1) separate gas/oil/water;

2) make sure oil and gas meet the requirements before being sent to refineries and natural-gas processing plants, respectively;

3) treat water before disposing or re-injecting it.

A processing plant complexity is defined by a reservoir technical and economic feasibility study. Therefore, a plant may or may not include only gas/oil/water separation, emulsion stabilization, gas compression and conditioning, oily water treatment, and water injection (SILVA et al., 2007).

Silva et al. (2007) shows a simplified scheme of a primary processing of fluids all the way from the underground reservoir to export and discard (Figure 22). The author also presents a couple possible plant arrangements as shown in Figure 23.

This study focuses in biphasic separator tanks, being the other equipment out of scope.

Figure 22 – Simplified primary processing plant.
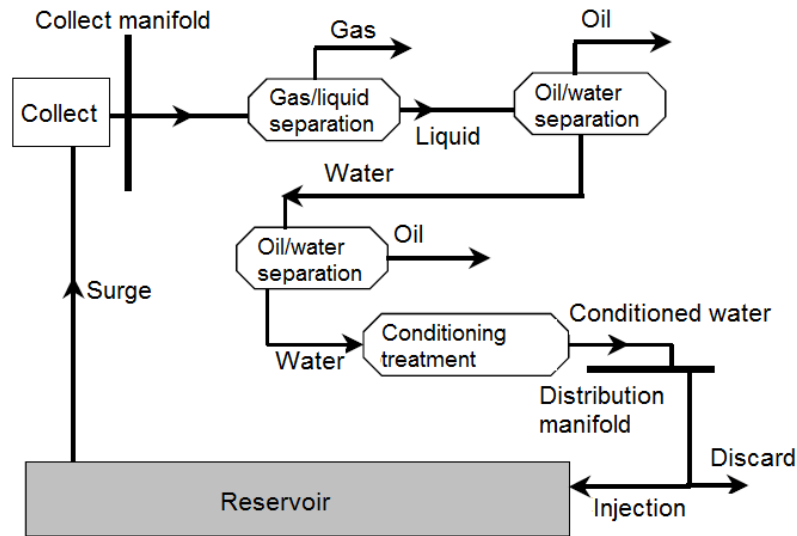
Source: adapted from SILVA et al. (2007).

Figure 23 – Different plant arrangements
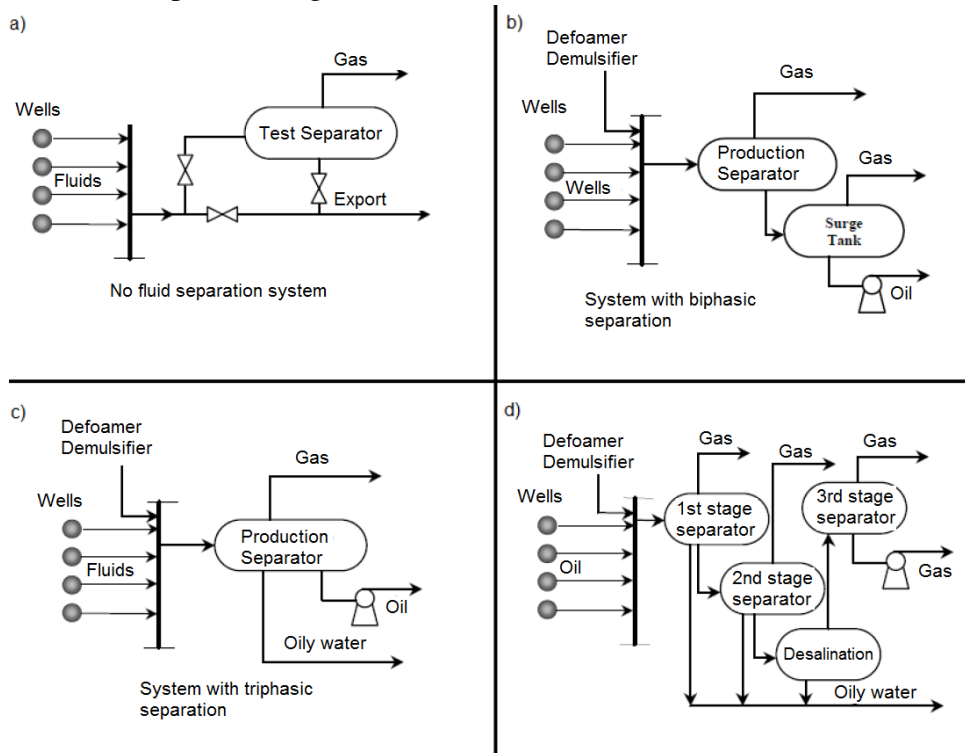
Source: adapted from SILVA et al. (2007).

2.7.3 Separator Tank

The separator tank is the first equipment in the primary processing plant, and the one that will receive the reservoir fluid mixture. It acts mainly by gravitational segregation, separating fluids by their density. Gas separates to the higher part of the tank and the liquids accumulate in the bottom part (SILVA et al., 2007). An example of a horizontal biphasic separator tank is shown in Figure 24.

Figure 24 – Horizontal biphasic separator tank.
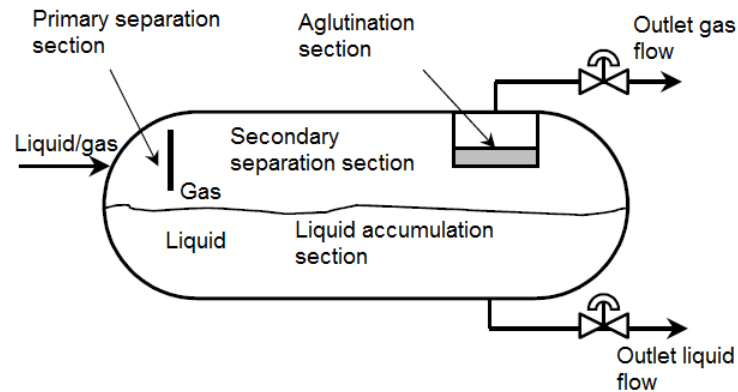
Source: adapted from SILVA et al. (2007).

The Primary Separation Section has a deflector ou difusing device that changes the fluid velocity abruptaly or makes it rotate, which will separate the components due to change in momentum. Liquid will accumulate in the Liquid Accumulation Section, where residual gas will still separate (SILVA et al., 2007).

Decantation occurs in the Seconday Separation Section, where larger liquid drops will fall from the gas. The gas will then pass through an Aglutination Section with mist extractor to retain remaining fluid in the gas phase (SILVA et al., 2007).

Separator tanks may be horizontal (Figure 24) or vertical (Figure 25). Horizontal separators have a better separation efficiency due to a larger interfacial area between gas and liquid and therefore are more common in higher Gas-Oil-Ratio (GOR) reservoirs. They are less efficient in getting rid of solids and in damping slug flow as demonstrated by Kindermann (2017).

Figure 25 – Vertical triphasic separator tank.
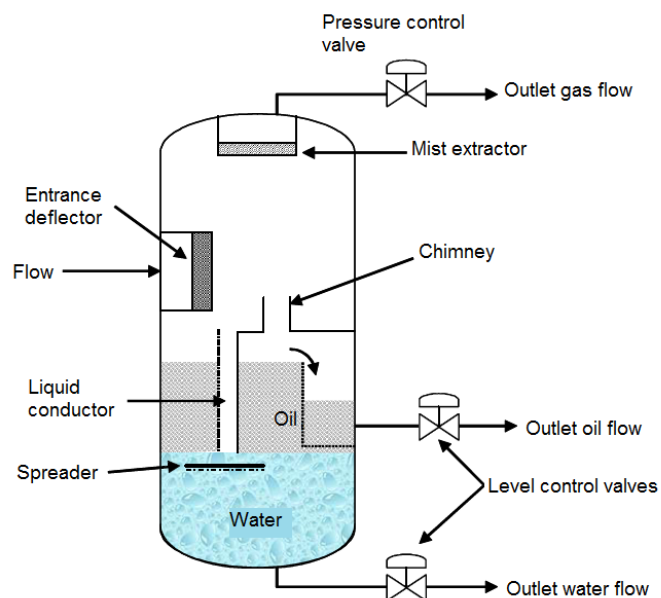
Source: adapted from SILVA et al. (2007).

2.7.4 Slug Flow

A slug is characterized by a liquid accumulation in a multiphasic flow and irregular gas and liquid flow and impulse variations through flowline sections (GODHAVN et al., 2004). Bai and Bai (2016) say that slug occurrance is the most important factor in guaranteeing of flow since pressure variations can be significative. This phenomenon floods and damages equipment. Therefore, equipment project should take this into account.

Bai and Bai (2016) classifies three types of slug flows: hydrodynamic slug, terrain-induced slug and operational-induced slug.

2.7.4.1 Hydrodynamic Slug

Occurs due to gas/liquid interfacial instability induced by flow conditions. When these conditions are met, the interface rises until the tubing ceiling, called Kelvin-Helmholtz wave. This structure is pushed by the gas phase as a slug due to a turbulent region formed behind it. This phenomenon is exemplified in Figure 26.

Figure 26 – Hydrodynamic slug.
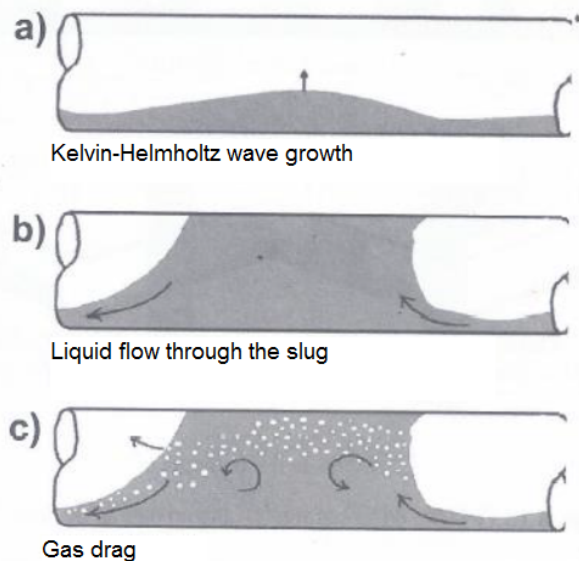
Source: adapted from BAI; BAI (2016).

2.7.4.2 Terrain-Induced Slug

Variations in underwater terrain may create geometries that induce slugs. An example is shown in Figure 27. First, liquid is accumulated in the tubing base. The fluid blocks the gas flow and pressure starts to build up. When the pressure reaches a critial value, the gas phase pushes the liquid phase violently as a slug.

Figure 27 – Terrain-induced slug

Slug formation   Slug development   Gas penetration   Gas purge
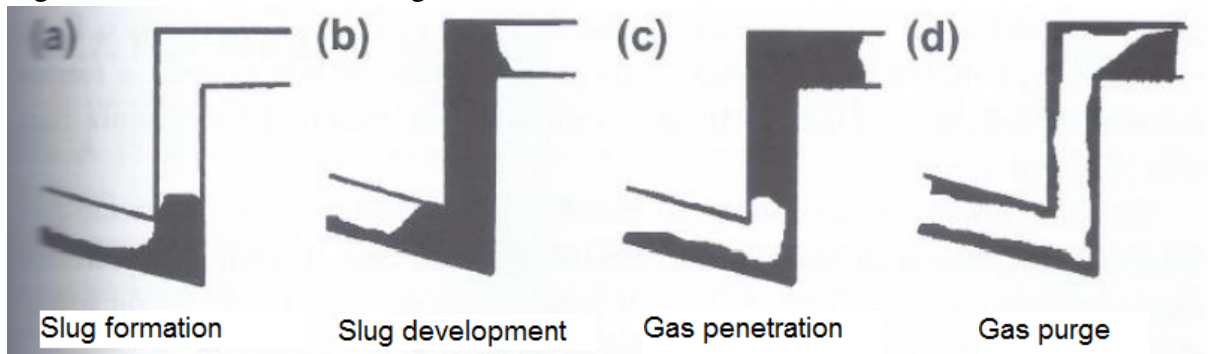
Source: adapted from BAI; BAI (2016).

2.7.4.3 Operational-Induces Slug

Occurs when changing operational conditions from steady state to transient. For instance, when doing PIG cleaning operations (BAI; BAI, 2016).

2.7.5 Slug Control

Previous researchers have studied ways to control slug flows. Godhavn et al. (2004) studied the effects of manipulating the choke valve when slugging exists in the pipeline with PI controllers arrangements which parameters are function of the slug density and volumetric flow. The authors' experiments presented an efficient control and managed to keep the controlled variables in the desired setpoints.

Stasiak et al. (2012) proposed a discrete PI controller on the choke valve in order to suppress oscillatory flow in risers using as parameters the oscillation frequency and sampling time. This method was simulated in the software OLGA and achieved the desired system stabilization.

Campos et al. (2015) developed a slug controller that acts with three modules: a Diagnostic Module that detect severe slugs, a Protection Module that prevents propagation of slug to topside equipment, and a Control Module that minimizes or eliminate the slugs keeping the choke valve at the desired position. An advanced controller is used in the project the method is applied to three offshore units. Major economic enhancements were reached by the implementation of this controller in the offshore units.

The aforementioned works control the intermittent flow by manipulating the choke valve. This work avoids manipulating the choke valve in order prevent eventual problems in other wells that may share the same subsea manifold.

2.8   OPTIMIZING FUNCTIONS

2.8.1   Conventional Methods

Conventional optimization methods are based in anaylizing analytically functions that describe a problem to find its maxima or minima. The next subsections explore one dimension derivative analysis, multidimensional derivative analysis and Lagrange multipliers.

2.8.1.1   One dimensional derivative

Stewart (2006) defines the absolute maximum of a function if there is a point c where $f(c) \geq f(x)$ for all given x in the function domain D. Similarly, an absolute minimum occurs when $f(c) \leq f(x)$ for every x in D. If instead of the domain D only the vicinities of c are analyzed, the previous statement defines local maximum and local minimum. Examples of maxima and minima are represented in Figure 28.

Figure 28 – Maxima and minima of an interval
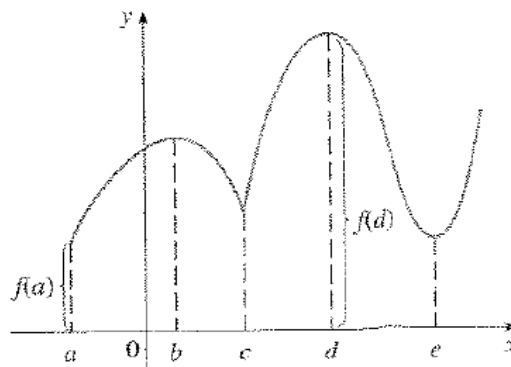
Source: STEWART (2006).

From Figure 28, it is possible to see that maxima and minima appear when

a) the derivative is zero (points b, d and e);

b) the derivative doesn't exist (point c); or

c) the point is in the limit of the interval (point a).

If a point meets any of the previous requirements, it is labeled as a critical number.

Therefore, Stewart (2006) suggests the following steps when looking for maxima and minima in an interval $[a,b]$:

1) find the critical numbers of f between $[a,b]$ and evaluate them;

2) evaluate the extremes of the interval;

3) the higher value is the absolute maximum and the lower value will be the absolute minimum of the interval.

2.8.2 Multi-dimensional derivative

Similarly to the previous subsection, Stewart (2007) defines a local maximum if $f(a,b) \geq f(x,y)$ when (x,y) is next to (a,b) and a local minimum if $f(a,b) \leq f(x,y)$ in the same condition. If this concept is extended to the whole domain of f, then the previous statement defines absolute maximum and minimum, respectively. Examples of local maxima and minima for a 3D function are shown in Figure 29.
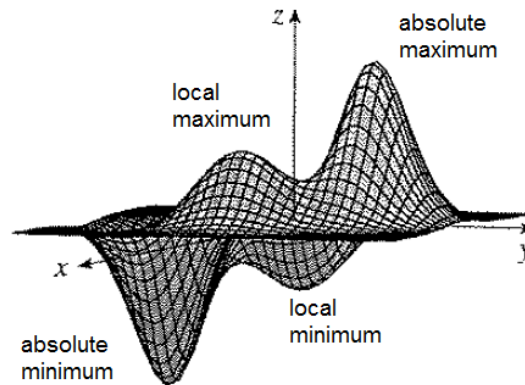
Figure 29 – Maxima and minima for a 3D function.

Source: adapted from STEWART (2007).

Stewart (2007) shows that if $f(a,b)$ is a local maximum or minimum and is derivatives exist, then $(\partial f/\partial x)_{(a,b)} = (\partial f/\partial y)_{(a,b)}$ and they are zero. Geometrically, this means that the tangent plan in this point is horizontal, as is possible to see intuitively from Figure 29. The author also provides a method to confirm if a critical number is a maximum or minimum based on the calculation of $D(a,b)$:

$$D(a,b) \triangleq \left\{ \frac{\partial^2 f}{\partial x^2} \frac{\partial^2 f}{\partial y^2} - \left[\frac{\partial^2 f}{\partial x \partial y} \right]^2 \right\}_{(a,b)}. \tag{2.80}$$

a) if $D > 0$ and $(\partial^2 f/\partial x^2)_{(a,b)} > 0$, then $f(a,b)$ is a local minimum;

b) if $D > 0$ and $(\partial^2 f/\partial x^2)_{(a,b)} < 0$, then $f(a,b)$ is a local maximum;

c) if $D < 0$, then $f(a,b)$ is neither a maximum or minimum.

Finding the absolute maximum and minimum within an interval is similar to the one-dimensional case. Critical numbers are evaluated and compared to each other and to the extreme values in the interval.

2.8.3 Lagrange Multipliers

Lagrange Multipliers method consists in finding maxima and minima of $f(x,y)$ with a constraint $g(x,y) = k$ (also applies for more dimensions). Geometrically, this means finding

a value c where the contour line $f(x,y) = c$ meets $g(x,y) = k$. In this point, vectors normal to (x_0, y_0) in both curves should be the same. This can be written mathematically as $\nabla f(x_0, y_0) = \lambda \nabla g(x_0, y_0)$ for a given λ (STEWART, 2007).

Example

Finding the maximum volume a cardboard box made from a 12m^2 sheet can have, with no lid. The box volume is $V(x,y,z) = xyz$ and the constraint is $g(x,y,z) = 2xz + 2yz + xy$, $g(x,y,z) = 12$, which is the sheet's area. The box is shown in Figure 30.

Figure 30 – Box without a lid made from a 12m^2 cardboard sheet cutout.
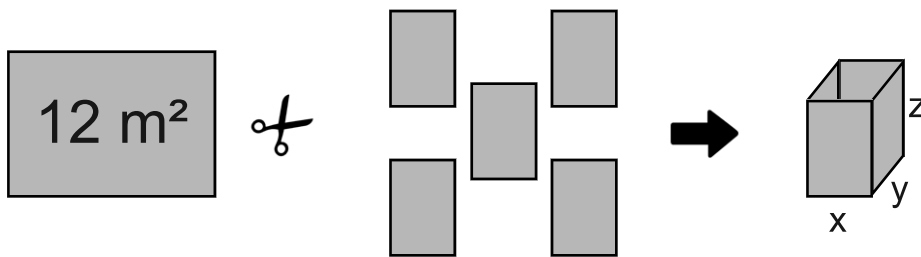
Equating $\nabla V = \lambda \nabla g$:

$$yz = \lambda(2z + y) \tag{2.81}$$

$$xz = \lambda(2z + x) \tag{2.82}$$

$$xy = \lambda(2x + 2y) \tag{2.83}$$

$$2xz + 2yz + xy = 12 \tag{2.84}$$

This system is solved by multiplying Equations 2.81, 2.82, and 2.83 by x, y, and z, respectively. Equating the resulting 2.81 and 2.82 gives $x = y$, and 2.82 and 2.83 gives $y = 2z$. Substituting $x = 2z$ and $y = 2z$ in Equation 2.84 gives $z = 1$ and therefore $x = 2$ and $y = 2$.

2.8.4 Metaheuristic Methods

Metaheuristic Methods, from *heuristicus* which means "to find" or "to discover" and *meta* which means "higher" or "beyond" (YANG, 2010), are often bio-inspired algorithms developed to solve complex and highly non-linear engineering problems. They are enhanced Heuristic methods, which are stochastic optimization approaches by trial and error. Metaheuristics add more randomization to the search and focus on intensification (exploitation) and diversification (exploration), combined with the selection of the best solutions in each iteration. A good

combination of these components usually ensures that the global optimality is achievable (YANG, 2010).

Some examples of Metaheuristic Methods are Ant Colony Optimization, Evolutionary Computation, Simulated Annealing, Particle Swarm Optimization, etc (BIANCHI et al., 2009). This work explores the Genetic Algorithm, which is a branch of evolutionary algorithms.

2.8.4.1 Genetic algorithm

Genetic Algorithms are inspired by natural selection, evolution, and molecular genetics. It is based on the four main pillars of evolution: population maintenance, diversity, natural selection and genetic heritage (FLOREANO; MATTIUSSI, 2008).

The algorithm initializes a population with several individuals, each one of them being a different attempt to solve a specific problem with a specific *fenotype* and a *genotype*. The fenotype is the evaluation of the problem itself, and the genotype is a genetic representation that will be inherited by future iterations (called *generations*), usually in a binary fashion. Links between genotype and fenotype can have several layers of complexity, from a direct link to sophisticated models. The genetic algorithm basically works in two steps: fenotype ranking and reproduction (FLOREANO; MATTIUSSI, 2008).

This method can be described as a simple iterative process with (1) an initialization step with a population of different individuals, (2) objective function evaluation for each individual, (3) individuals with better fenotypes are selected whilst the worst ones go extinct, (4) surviving individuals reproduce proportionally to their score, (5) individuals share information (*crossover*) and random mutations may occur in random individuals, generating a new population of different individuals, (6) repeats from step 2. Floreano and Mattiussi (2008) ilustrate this simplified scheme in Figure 31.

When construction a genetic model, the main topics to take into account are:

1) choosing a genetic representation for the individuals;

2) how to initialize the first population;

3) define the objective funtion to be minimized;

4) define the selection operator;

5) define the crossover operator;

6) define the mutation operator;

7) plan a data analysis procedure.

Creating a genetic model from scratch is out of the scope of this work, but Floreano and Mattiussi (2008) explore these steps in detail. This work uses the genetic algorithm function "*ga*" already available in (MATLAB, 2009).

Figure 31 – Simple genetic algorithm.
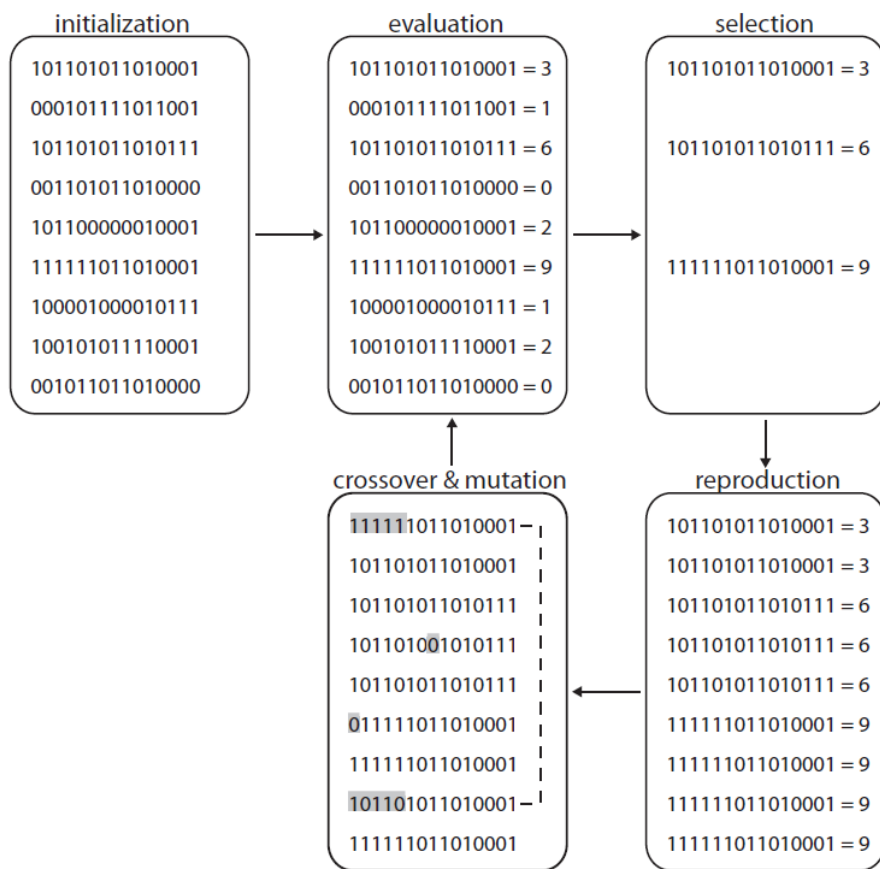
Source: FLOREANO; MATTIUSSI (2008).

3 METHODOLOGY

3.1 DYNAMIC MODEL

In this section, the biphasic separator tank is modeled step-by-step as presented by Nunes et al. (2010).

3.1.1 Valves

Valves are used to control process variables and should be automatically and remotely operated. Their action is either pneumatic, piston, hydraulic or electrohydraulic.

Valves are classified as rotative and linear. Rotative valves have an obturator that rotates, changing the flow. They are commonly used in dirty fluids. Linear valves obturator translates instead of rotate, controlling the flow by sealing its passage.

3.1.1.1 Flow through the valve

Assuming a tank in Figure 1 (presented below again), take two points: one upstream (1) and the other downstream (2) a valve that produces the flow q. Using Bernoulli's equation, it is true that

$$\frac{v_1^2}{2} + gh_1 + \frac{P_1}{\rho} = \frac{v_2^2}{2} + gh_2 + \frac{P_2}{\rho}, \tag{3.1}$$
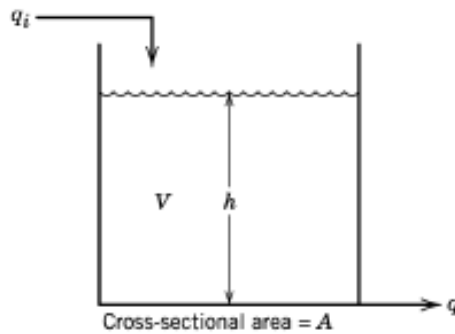
Source: SEBORG et al. (2011).

where v is the fluid velocity in the specific point, h its height, P its pressure, ρ its density, and g the gravity constant. Since both points have the same height, these terms cancel out. The difference between their pressures is defined as ΔP, and the upstream point is assumed to have no velocity, that is, $v_1 = 0$. Therefore,

$$v_2^2 = \frac{2\Delta P}{\rho}, \tag{3.2}$$

which can be written as

$$v_2^2 \propto \Delta P. \tag{3.3}$$

Since velocity itself is proportional to volumetric flow,

$$q^2 \propto \Delta P, \tag{3.4}$$

which is, in fact

$$F \triangleq q = c_v f(x_v) \sqrt{\Delta P / \rho_f}, \tag{3.5}$$

where c_v is the valve flow coefficient in GPM/$\sqrt{\text{psi}}$, $f(x_v)$ is the dimensionless flow characteristic curve, x_v is the valve opening fraction, ΔP is the pressure drop throughout the valve in psi, and ρ_f is the relative fluid density (fluid density divided by water density).

From Nunes et al. (2010), gas flow through the valve is

$$F = c_v f(x_v) \sqrt{P_1 \Delta P / (\rho_f T_f)}, \tag{3.6}$$

where T_f is the gas temperature and P_1 is the upstream valve pressure, that is, the pressure inside the separator tank.

The valve characteristic flow curve $f(x_v)$ is a function of its components. Nunes et al. (2010) present the following models:

Square Root
$$f(x_v) = \sqrt{x_v}; \tag{3.7}$$

Linear
$$f(x_v) = x_v; \tag{3.8}$$

Percentage
$$f(x_v) = R^{(x_v - 1)}; \tag{3.9}$$

Hyperbolic
$$f(x_v) = [R - (R - 1)x_v]^{-1}; \tag{3.10}$$

Fast action
$$f(x_v) = \exp(x_v), \tag{3.11}$$

where R is the valve rangeability, that is, the relationship between the maximum and minimum flow it allows. In this work, the linear characteristic flow curve is used.

Poligon Válvulas Industriais (2014) suggests an ideal opening fraction operation ranging from 30% to 80%, where flow behavior is nearly linear and optimal for process control and stability.

3.1.2 Tank

For a horizontal cylindrical tank with length C and diamater D (Figure 32), the relationship of its fluid volume V and fluid level h is derived analyzing the triangle formed between the fluid level and the tank center.

Figure 32 – Cylindrical tank model
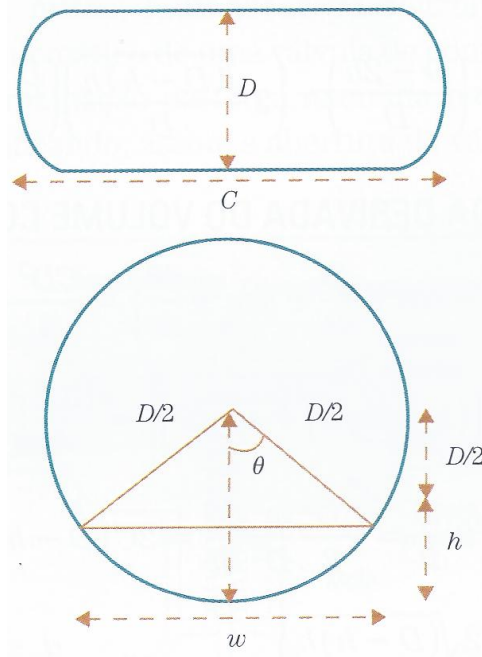
Source: NUNES et al. (2010).

The circle section area is defined by

$$A_{section} = \frac{\theta D^2}{4},$$
(3.12)

and the triangle area is

$$A_{triangle} = \left(\frac{D}{2} - h\right)\frac{D}{2}\sin\theta.$$
(3.13)

From Figure 32, it is possible to see that

$$\frac{D}{2}\cos\theta = \frac{D}{2} - h,$$
(3.14)

which can be rearranged to

$$\theta = \arccos\left(\frac{D - 2h}{D}\right).$$
(3.15)

Also, applying the Pithagorean theorem, $\sin\theta$ is calculated by

$$\left(\frac{D}{2}\right)^2 = \left(\frac{D}{2} - h\right)^2 + \left(\frac{D}{2}\sin\theta\right)^2,$$
(3.16)

$$\sin\theta = \frac{2\sqrt{(D-h)h}}{D} \tag{3.17}$$

Finally, applying Equations 3.15 and 3.17 in Equations 3.12 and 3.13, respectively, and subtracting them provides

$$
\begin{aligned}
A \quad &= \arccos\left(\frac{D-2h}{D}\right)\frac{D^2}{4} - \left(\frac{D-2h}{2}\right)\frac{D}{2}\left(2\frac{\sqrt{(D-h)h}}{D}\right) \\
&= \frac{D^2}{4}\left[\arccos\left(\frac{D-2h}{D}\right) - \left(2\frac{\sqrt{(D-h)h}}{D}\right)\left(\frac{D-2h}{D}\right)\right].
\end{aligned}
\tag{3.18}
$$

To calculate the volume, Equation 3.18 is multiplied by the length C,

$$V = \frac{CD^2}{4}\left[\arccos\left(\frac{D-2h}{D}\right) - \left(2\frac{\sqrt{(D-h)h}}{D}\right)\left(\frac{D-2h}{D}\right)\right], \tag{3.19}$$

and its derivative in respect to time is

$$\frac{dV}{dt} = 2C\sqrt{(D-h)h}\frac{dh}{dt}. \tag{3.20}$$

Liquid and gas phases are modeled by conservation of mass, as follows.

3.1.2.1 Liquid Phase

Conservation of mass starts with the concept of Equation 2.18,

$$\frac{dM_L(t)}{dt} = [L_{in}(t) - L_{out}(t)]\rho_L, \tag{3.21}$$

where $M_L(t)$ is the mass of liquid inside the tank, $L_{in}(t)$ is the inlet liquid volumetric flow over time, $L_{out}(t)$ is the outlet liquid volumetric flow over tive through the valve, and ρ_L is the liquid's density, assumed to be constant. The left hand side of Equation 3.21 is the derivative of fluid volume in respect to time multiplied by its density, which from Equation 3.20 becomes

$$\frac{dh_L(t)}{dt} = \frac{L_{in}(t) - L_{out}(t)}{2C\sqrt{[D - h_L(t)]h_L(t)}}. \tag{3.22}$$

Labeling the right hand side of Equation 3.22 as f, the model is linearized as

$$\frac{dh'_L(t)}{dt} = \left.\frac{\partial f}{\partial L_{in}}\right|_{SS} L'_{in} + \left.\frac{\partial f}{\partial L_{out}}\right|_{SS} L'_{out} + \left.\frac{\partial f}{\partial h_L}\right|_{SS} h'_L. \tag{3.23}$$

Since $L_{out}(t)$ is the liquid flow through the valve, it is then described by Equation 3.5, and Equation 3.23 is rewritten as

$$\frac{dh'_L(t)}{dt} = \left.\frac{\partial f}{\partial L_{in}}\right|_{SS} L'_{in} + \left.\frac{\partial f}{\partial L_{out}}\right|_{SS}\left(\left.\frac{\partial L_{out}}{\partial x_L}\right|_{SS} x'_L + \left.\frac{\partial L_{out}}{\partial P}\right|_{SS} P' + \left.\frac{\partial L_{out}}{\partial h_L}\right|_{SS} h'_L\right) + \left.\frac{\partial f}{\partial h_L}\right|_{SS} h'_L. \tag{3.24}$$

Applying Lalace Transform in both sides and solving for $H'(s)$ results in three transfer functions:

$$G_1 := \frac{H'(s)}{L'_{in}(s)} = \frac{K_1}{\tau_L s + 1};$$

$$G_2 := \frac{H'(s)}{X'_L(s)} = \frac{K_2}{\tau_L s + 1};$$

(3.25)

$$G_3 := \frac{H'(s)}{P'(s)} = \frac{K_3}{\tau_L s + 1},$$

where the aforementioned constants are

$$\tau_L = -\left(\frac{df}{dh_L} + \frac{df}{dL_{out}}\frac{dL_{out}}{dh_L}\right)^{-1}_{SS} \quad ; \quad K_1 = \tau_L \left.\frac{df}{dL_{in}}\right|_{SS};$$

$$K_2 = \tau_L \left(\frac{df}{dL_{out}}\frac{dL_{out}}{dx_L}\right)_{SS} \quad ; \quad K_3 = \tau_L \left(\frac{df}{dL_{out}}\frac{dL_{out}}{dP}\right)_{SS}.$$

(3.26)

3.1.2.2 Gas Phase

Similarly to the liquid phase, conservation of mass to the gas phase starts as

$$\frac{dM_G(t)}{dt} = [G_{in}(t) - G_{out}(t)]\rho_G(t),$$

(3.27)

where $M_G(t)$ is the mass of gas inside the tank, $G_{in}(t)$ is the inlet gas volumetric flow, $G_{out}(t)$ is the outlet gas volumetric flow, and $\rho_G(t)$ is the gas density.

Assuming ideal gas behavior, the left hand side of Equation 3.27 can be rewritten as

$$\frac{dM_G(t)}{dt} = \frac{MM}{R_G T}\left[V_G(t)\frac{dP(t)}{dt} + P(t)\frac{dV_G(t)}{dt}\right],$$

(3.28)

being MM the gas molar mass, T the gas temperature, R_G is the universal gas constant, and $P(t)$ the gas pressure inside the tank. Since the tank volume is constant, $dV_G(t)/dt = -[L_{in}(t) - L_{out}(t)]$. Equating 3.27 and 3.28 results in

$$\frac{dP(t)}{dt} = \frac{P(t)[G_{in}(t) - G_{out}(t) + L_{in}(t) - L_{out}(t)]}{V - V_L(t)}.$$

(3.29)

Labeling the right hand side of Equation 3.29 as g and linearizing it provides

$$\frac{dP'(t)}{dt} = \left.\frac{\partial g}{\partial P}\right|_{SS}P' + \left.\frac{\partial g}{\partial G_{in}}\right|_{SS}G'_{in} + \left.\frac{\partial g}{\partial G_{out}}\right|_{SS}G'_{out} + \left.\frac{\partial g}{\partial L_{in}}\right|_{SS}L'_{in} + \left.\frac{\partial g}{\partial L_{out}}\right|_{SS}L'_{out} + \left.\frac{\partial g}{\partial V_L}\right|_{SS}V'_L.$$

(3.30)

Again, $L_{out}(t)$ is described by Equation 3.5, $G_{out}(t)$ by Equation 3.6 and V_L by Equation 3.19. Equation 3.30 becomes

$$
\begin{aligned}
\frac{dP'(t)}{dt} = \;& \frac{\partial g}{\partial P}\bigg|_{SS} P' + \frac{\partial g}{\partial G_{in}}\bigg|_{SS} G'_{in} + \frac{\partial g}{\partial G_{out}}\bigg|_{SS} \left(\frac{\partial G_{out}}{\partial x_G}\bigg|_{SS} x'_G + \frac{\partial G_{out}}{\partial P}\bigg|_{SS} P' + \frac{\partial G_{out}}{\partial T}\bigg|_{SS} T' \right) + \\[2mm]
& \frac{\partial g}{\partial L_{in}}\bigg|_{SS} L'_{in} + \frac{\partial g}{\partial L_{out}}\bigg|_{SS} \left(\frac{\partial L_{out}}{\partial x_L}\bigg|_{SS} x'_L + \frac{\partial L_{out}}{\partial P}\bigg|_{SS} P' + \frac{\partial L_{out}}{\partial h_L}\bigg|_{SS} h'_L \right) + \\[2mm]
& \left(\frac{\partial g}{\partial V_L} \frac{\partial V_L}{\partial h_L} \right)_{SS} h'_L.
\end{aligned}
$$

(3.31)

Applying Laplace Transform and solving for $P'(s)$ yields six more transfer functions:

$$
G_4 := \frac{P'(s)}{L'_{in}(s)} = \frac{K_4}{\tau_G s + 1}; \quad G_7 := \frac{P'(s)}{H'_L(s)} = \frac{K_7}{\tau_G s + 1};
$$

$$
G_5 := \frac{P'(s)}{G'_{in}(s)} = \frac{K_5}{\tau_G s + 1}; \quad G_8 := \frac{P'(s)}{X'_G(s)} = \frac{K_8}{\tau_G s + 1}; \tag{3.32}
$$

$$
G_6 := \frac{P'(s)}{X'_L(s)} = \frac{K_6}{\tau_G s + 1}; \quad G_9 := \frac{P'(s)}{T'(s)} = \frac{K_9}{\tau_G s + 1},
$$

and the constants are

$$
\tau_G = -\left(\frac{dg}{dP} + \frac{dg}{dL_{out}}\frac{dL_{out}}{dP} + \frac{dg}{dG_{out}}\frac{dG_{out}}{dP} \right)^{-1}_{SS};
$$

$$
K_4 = \tau_G \frac{dg}{dL_{in}}\bigg|_{SS} \quad ; \quad K_5 = \tau_G \frac{dg}{dG_{in}}\bigg|_{SS};
$$

(3.33)

$$
K_6 = \tau_G \left(\frac{dg}{dL_{out}}\frac{dL_{out}}{dx_L} \right)_{SS}; \quad K_7 = \tau_G \left(\frac{dg}{dL_{out}}\frac{dL_{out}}{dh_L} + \frac{dg}{dV_L}\frac{dV_L}{dh_L} \right)_{SS};
$$

$$
K_8 = \tau_G \left(\frac{dg}{dG_{out}}\frac{dG_{out}}{dx_G} \right)_{SS}; \quad K_9 = \tau_G \left(\frac{dg}{dG_{out}}\frac{dG_{out}}{dT} \right)_{SS}.
$$

3.1.3 Model Diagram

From Equations 3.25 and 3.32, liquid level and gas pressure behavior in Laplace domain can be written as

$$
H'_L(s) = G_1 L'_{in}(s) + G_2 X'_L(s) + G_3 P'(s);
$$

(3.34)

$$
P'(s) = G_4 L'_{in}(s) + G_5 G'_{in}(s) + G_6 X'_L(s) + G_7 H'_L(s) + G_8 X'_G(s) + G_9 T'(s).
$$

Since particular variables can be set constant while studying other variables (Section 2.2.2), the disturbance variables $L'_{in}(s)$ and $G'_{in}(s)$ are set to zero. Also, Nunes et al. (2010) assume isothermal behavior, resulting in $T'(s)$ also zero:

$$H'_L(s) = G_2 X'_L(s) + G_3 P'(s);$$

(3.35)

$$P'(s) = G_6 X'_L(s) + G_7 H'_L(s) + G_8 X'_G(s).$$

Equating liquid level and gas pressure from 3.35 results in

$$H'_L(s) = \left[\frac{G_2 + G_3 G_6}{1 - G_3 G_7}\right] X'_L(s) + \left[\frac{G_3 G_8}{1 - G_3 G_7}\right] X'_G(s),$$

(3.36)

$$P'(s) = \left[\frac{G_6 + G_2 G_7}{1 - G_3 G_7}\right] X'_L(s) + \left[\frac{G_8}{1 - G_3 G_7}\right] X'_G(s),$$

which can be further simplified to

$$H'_L(s) = G_{p11} X'_L(s) + G_{p12} X'_G(s),$$

(3.37)

$$P'(s) = G_{p21} X'_L(s) + G_{p22} X'_G(s).$$

These transfer functions are then transcribed as a block diagram in the same fashion as Figure 15

The setpoints for liquid level and gas pressure are located in the left-hand side of Figure 33 (which are zero since disturbance variables are being used). Saturation blocks for the valves were implemented to assure their opening fractions will not exceed the realm of physical possibilites. Controller blocks are regular parallel PID controllers, described as

$$G_c = K_c \left[1 + \frac{1}{\tau_I s} + \tau_D s\right].$$

(2.57)

Next there are the four transfer functions from Equations 3.37 and the closed loops. There are four output variables in this diagram, which are $X'_L(s)$ and $X'_G(s)$ roughly in the center, and $H'(s)$ and $P'(s)$ to the right.

3.2 OPTIMIZATION

3.2.1 Fitness Function, Parameters and Constraints

Fitness function

The GA works to minimize the maximum deviation ratio of liquid level, gas pressure, valves opening fraction and outlet liquid flow, that is, the greater of them all. This function is represented by Equation 3.38.

$$\text{fitness} = \max\left(\left|\frac{h'(t)}{\bar{h}_L}\right|, \left|\frac{P'(t)}{\bar{P}}\right|, \left|\frac{x'_L(t)}{\bar{x}_L}\right|, \left|\frac{x'_G(t)}{\bar{x}_G}\right|, \left|\frac{L'_{out}(t)}{\bar{L}_{out}}\right|\right),$$

(3.38)

Figure 33 – Model block diagram
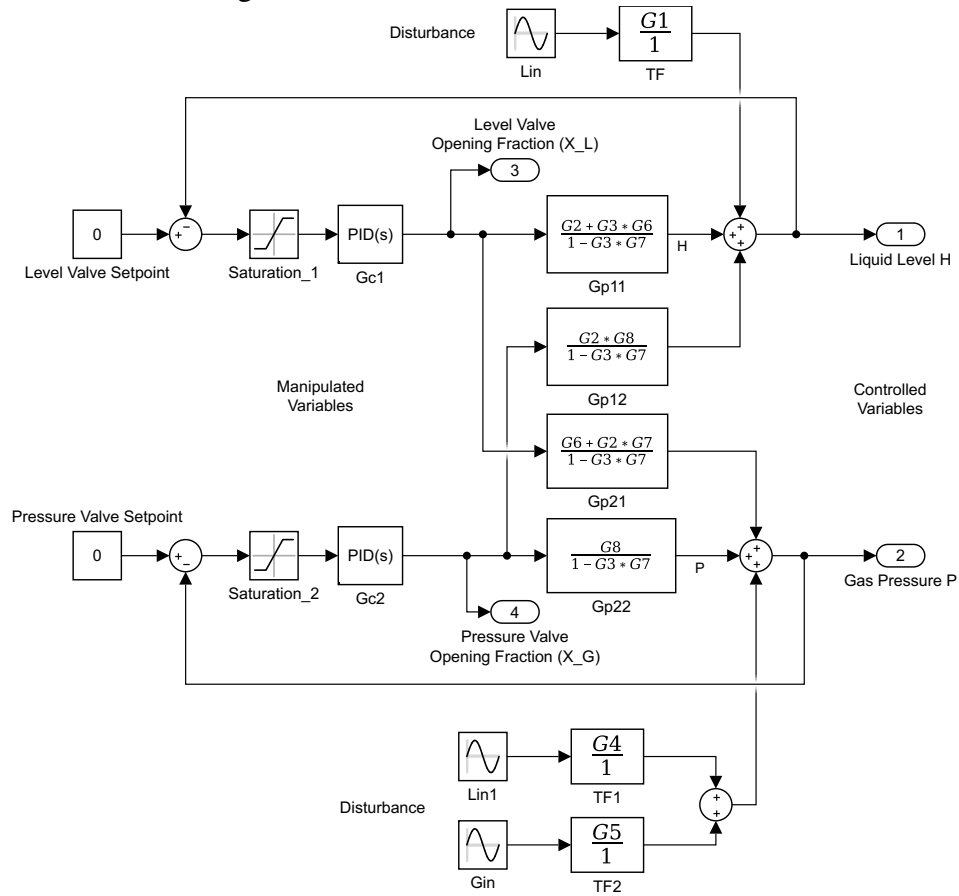
Source: adapted from KINDERMANN (2017).

where a bar over a variable indicates steady state value (see Table 2).

Parameters and constraints

The optimization aims at minimizing the fitness function by finding optimal PID parameters to G_{c1} and G_{c2} (see Figure 33). Equation 2.57 can be rewritten as

$$G_c = K_p + \frac{I}{s} + \tau_D \frac{N}{1 + N\frac{1}{s}}, \tag{3.39}$$

for both liquid and gas valve controllers. N is equivalent to the derivative filter and its default value is 100. All parameters are constrained to the interval [-10,10].

3.2.2 Genetic algorithm parameters

This work uses the "*ga*" genetic algorithm function available in MATLAB (2009). This function receives several parameters, for instance functions to generate the initial population, mutation functions, crossover functions, and much more. Most of them are kept default, changing only the following inputs:

Table 1 – GA parameters

Parameter	Input
Population (Individuals)	50
Generations	30
Mutation Function	*@mutationadaptfeasible*
Plot Function	*@gaplotbestf*

Population is the number of solutions the algorithm generates in each iteration. Generations is the number of iterations the algorithm will simulate. The Mutation Function dictates how mutation occurs. In this case, *@mutationadaptfeasible* is used to keep mutations within the bounded interval. The plot function determines what will be plotted. In this work, *@gaplotbestf* plots the minimum and average function values for each generation.

3.3   INITIALIZATION

Steady state values are presented in Table 2 according to Kindermann (2017), Nunes et al. (2010) and tanks catalogues. Length C and diameter D values were calculated by Kindermann (2017) when optimizing a biphasic separator tank geometry to level and pressure control purposes. The author optimized the ratio C/D, bounded by [2,15] with a Particle Swarm Optimization (PSO) algorithm, resulting $C/D = 2.0258$. Applying this ratio to a volume of $V = 19.8 m^3$ results in $C = 4.7m$ and $D = 2.3m$.

Table 2 – Steady state values

Variable name	Symbol	Value	Unit
Liquid valve downstream pressure	P_1	1.5	bar
Gas valve downstream pressure	P_2	6	bar
Liquid valve flow constant	C_{VL}	1025	GPM/$\sqrt{\text{psi}}$
Gas valve flow constant	C_{VG}	120	GPM/$\sqrt{\text{psi}}$
Liquid density	ρ_L	850	kg/m^3
Water density	$\rho_{H_2O,15.5^oC}$	999.19	kg/m^3
Tank volume	V	19.8	m^3
Tank length	C	4.7	m
Tank diameter	D	2.3	m
Gravity	g	9.81	m/s^2
Gas molar mass	MM_G	0.021	kg/mol
Air molar mass	MM_{air}	0.02897	kg/mol
Temperature	T	303.15	K
Inlet liquid flow	$\bar{L}_{in}$	0.08	m^3/s
Outlet liquid flow	$\bar{L}_{out}$	0.08	m^3/s
Inlet gas flow	$\bar{G}_{in}$	0.16	m^3/s
Outlet gas flow	$\bar{G}_{out}$	0.16	m^3/s
Tank pressure	$\bar{P}$	8	bar
Liquid Level	$\bar{h}_L$	1.1	m
Liquid valve opening fraction	$\bar{x}_L$	0.5	-
Gas valve opening fraction	$\bar{x}_G$	0.5	-

Disturbance variables $L'_{in}(t)$ and $G'_{in}(t)$ are the ones used by Kindermann (2017), described by

$$L'_{in}(t) = -0.03 + 0.05 \sin\left(\frac{2\pi t}{1320}\right),$$

$$G'_{in}(t) = -0.0673 + 0.0928 \sin\left(\frac{2\pi t}{1320}\right).$$

(3.40)

These equations are simple slug flow simulations taken from real data, transformed into percentual variation and applied to the flow values from Table 2. These disturbances are multiplied by their respective transfer functions in Equation 3.34 and then added to the sum points in Figure 33. Simulation time is set to 30000 seconds (500 minutes).

4 RESULTS AND DISCUSSION

In this section, the optimization results are presented with a briefly explanation and then compared to a previous experiment performed by Kindermann (2017) over the same physical model.

The GA optimization converged to the PID values and maximum percent deviations shown in Table 3.

Table 3 – Simulation results

	Liquid			Gas	
K_{p1}	=	-1.7658	K_{p2}	=	-0.0999
I_1	=	-5.0552	I_2	=	-0.4839
τ_{D_1}	=	0.2224	τ_{D_2}	=	2.5630
Maximum Deviations					
Outlet liquid flow		=		375.8310 %	
Valve opening fraction		=		51.9985 %	
Pressure		=		8.5134 %	
Level		=		0.4322 %	

Best and mean fitness values for every generation are shown in Figure 34. The code is written in a way that if the simulation can not converge due to any of the PID values, the fitness is set to infinity for natural selection purposes. From Figure 34 it is possible to see that at least one individual from each generation causes simulation divergence, hence all mean values being off chart (Inf). Outlet liquid flow, valves opening fraction, liquid level and gas pressure behavior over time for the optimized solution are shown in Figure 35 and Figure 36. Level and pressure deviation values in Table 3 correspond to peaks in the very beginning of the simulated time, but the oscillations actually provide even smaller values.

Figure 34 – Fitness evolution over the generations.

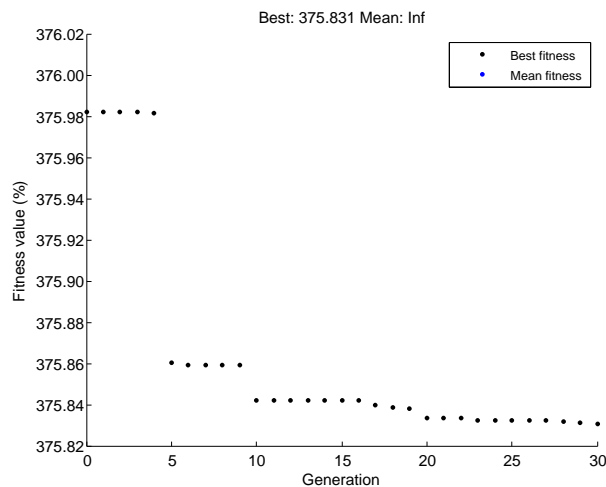Figure 35 – (a) Outlet liquid flow deviation, (b) Valves opening fraction.

(a)   (b)
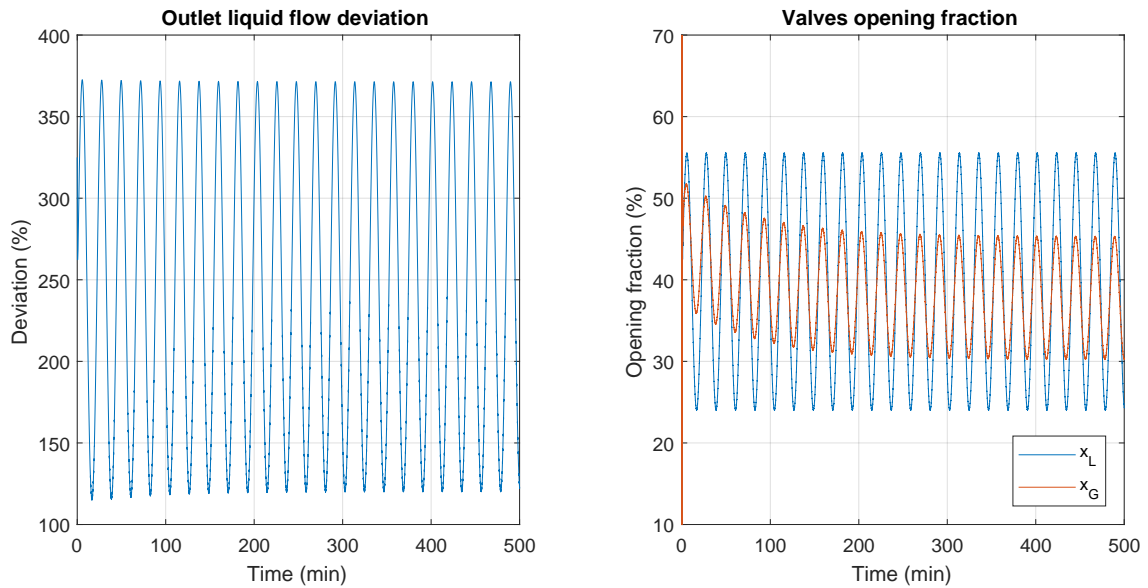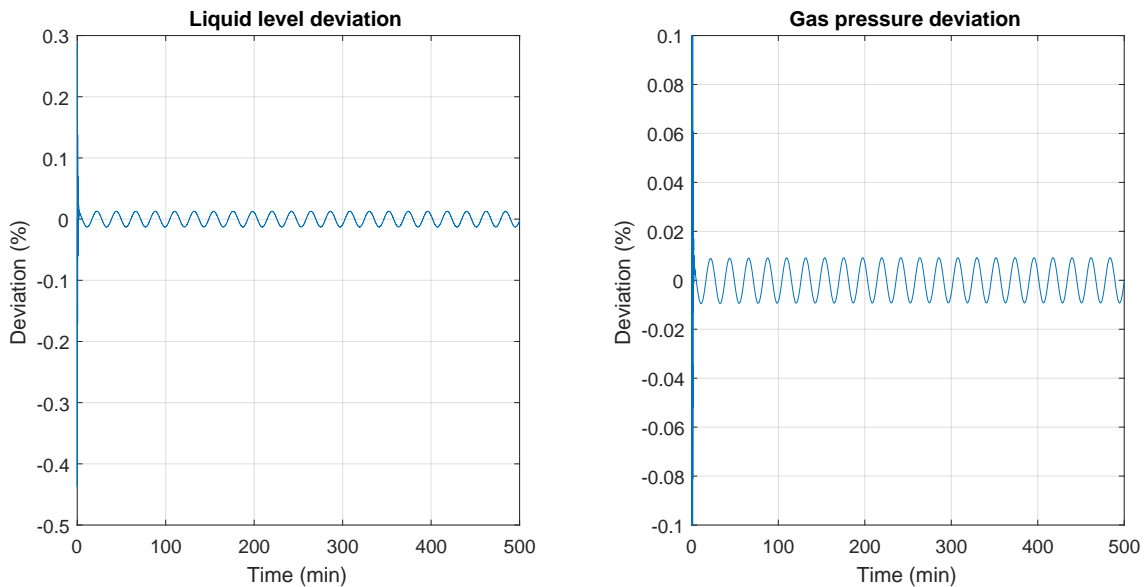
Figure 36 – (a) Level deviation, (b) Pressure deviation.

(a)   (b)

Outlet liquid flow amplitude in Figure 35 is unacceptably high, suggesting this may not be an optimal method to control slug flows. The outlet flow curve can be described by

$$L_{out} = 0.2705 + 0.1073 \sin\left(\frac{2\pi}{1320}t\right). \tag{4.1}$$

When compared to Equation 3.40, it is possible to see a roughly 100% amplification in its amplitude while keeping the same frequency.

Valve opening fractions in Figure 35 are generally good despite the liquid valve exceeding 5% from the lower limit suggested by Poligon Válvulas Industriais (2014). The oscillation amplitude is within acceptable limits. It is clear from Figure 36 that this solution is highly efficient in controlling liquid level and gas pressure since they have barely changed at all. An odd behavior occurs right in the beginning of the simulated time with higher amplitude but it is still within safe limits.

A previous study performed by Kindermann (2017) optimized the same system with two proportional controllers and a Particle Swarm Optimization (PSO) meta-heuristic algorithm, arbitrarily labeled as PSO-P arrangement. These results are compared with this work in the next figures and table.

Figure 37 – Outlet liquid flow deviation. (a) PSO-P, (b) GA-PID.
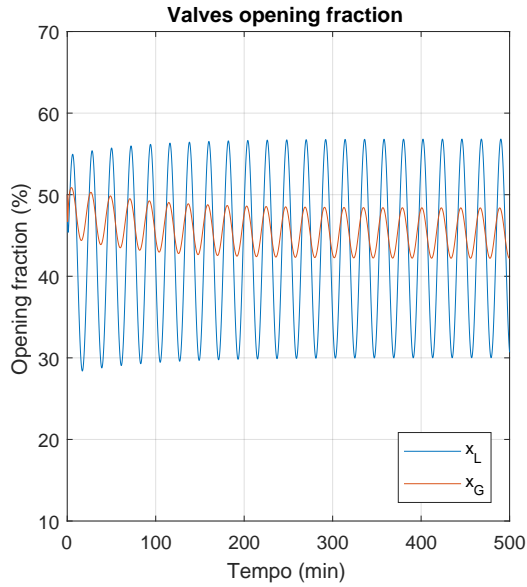(a)   (b)
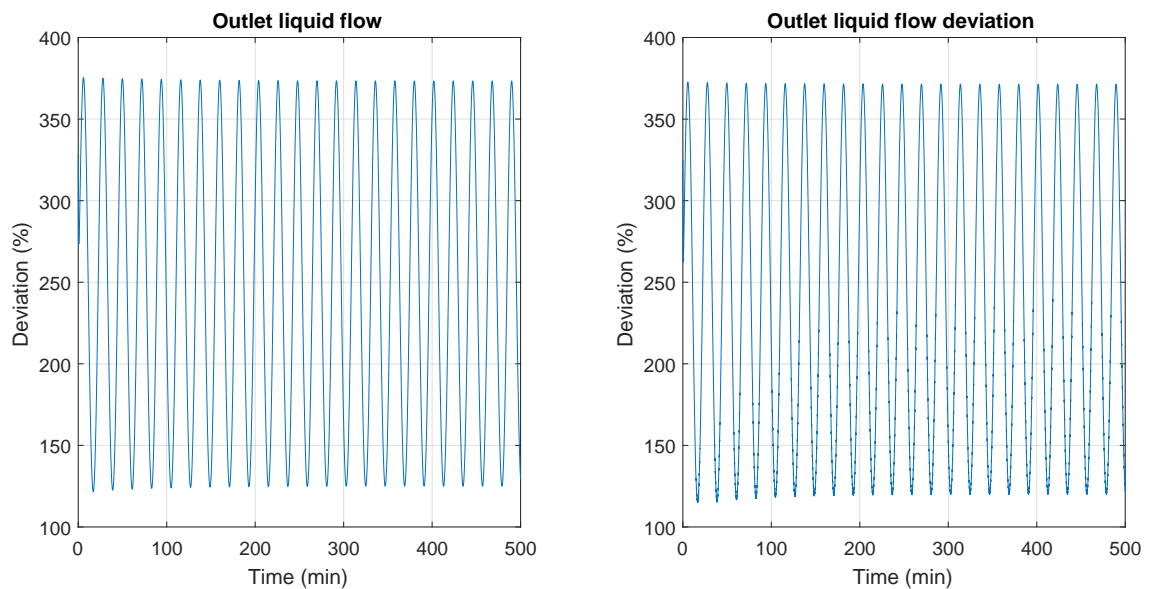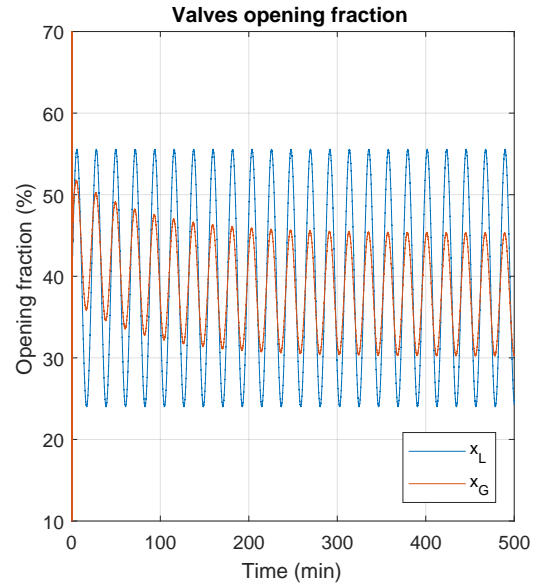

Source: adapted from Kindermann, 2017

Figure 38 – Valves opening fractions. (a) PSO-P, (b) GA-PID.
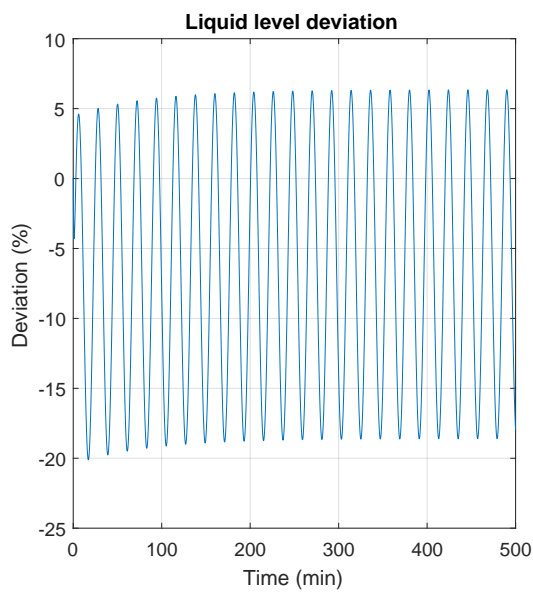(a)   (b)
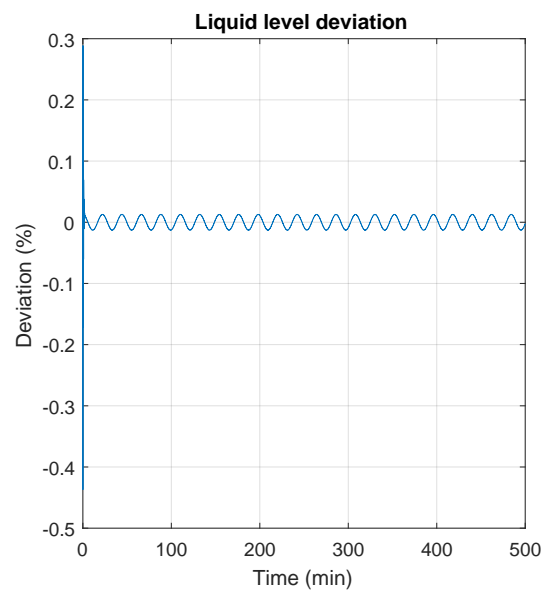

Source: adapted from Kindermann, 2017

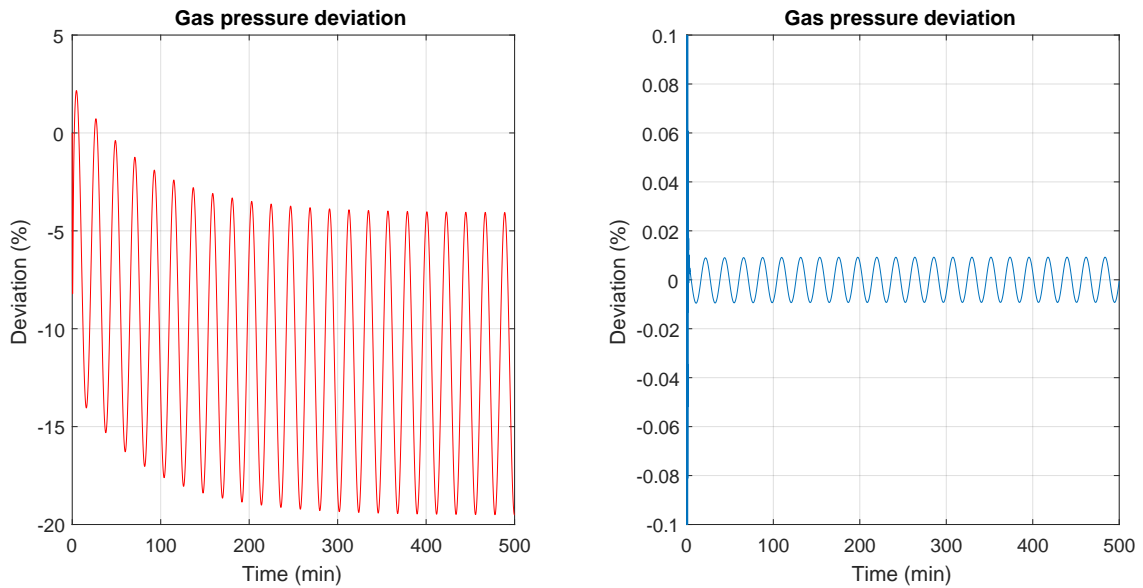Figure 39 – Level deviation. (a) PSO-P, (b) GA-PID.
(a)   (b)

Source: adapted from Kindermann, 2017

Figure 40 – Pressure deviation. (a) PSO-P, (b) GA-PID.
(a)   (b)

Source: adapted from Kindermann, 2017

Table 4 – PSO-P vs GA-PID

Maximum Deviations	PSO-P	GA-PID
Outlet	375.44%	375.83%
Valves opening fraction	40.00%	52.00%
Liquid level	18.61%	0.43%
Gas pressure	19.52%	8.51%

From this comparison, it is possible to see that the GA-PID arrangement performs better in controlling liquid level and gas pressure compared to the PSO-P experiment. Outlet liquid flow is kept the same in both studies. PSO-P had a better control over the valves opening fraction amplitudes keeping them within the optimal range provided by Poligon Válvulas Industriais (2014).

Difference in control performance may be due to the different metaheuristic approach chosen and/or the change from a Proportional to a PID controller, the latter being more likely to be true. Since the GA does not have a defined path to follow in the sense that it is not derivative based, there is no absolute guarantee that a global solution has been obtained (ARORA, 2004). When the fitness function does not improve any further, it is hard to tell if it has reached the optimal result or if it is stuck in a local optimum. In the latter case, the algorithm depends on random mutations to find new solutions and this may take several generations to happen (FLOREANO; MATTIUSSI, 2008). On the other hand, there is evidence that PSO performs better then other optimization techniques when optimizing real functions (FLOREANO; MATTIUSSI, 2008). Therefore, the difference in results is probably due to the PID controller performance.

The simulation is run a couple more times. First, the controller is kept off until 250 minutes. The graphs of Figures 41 and 42 show how differently the system responds to the slug flow before and after the controllers are turned on.

Figure 41 – Before and after turning the controller on: (a) Liquid level, (b) Gas pressure.
(a)   (b)
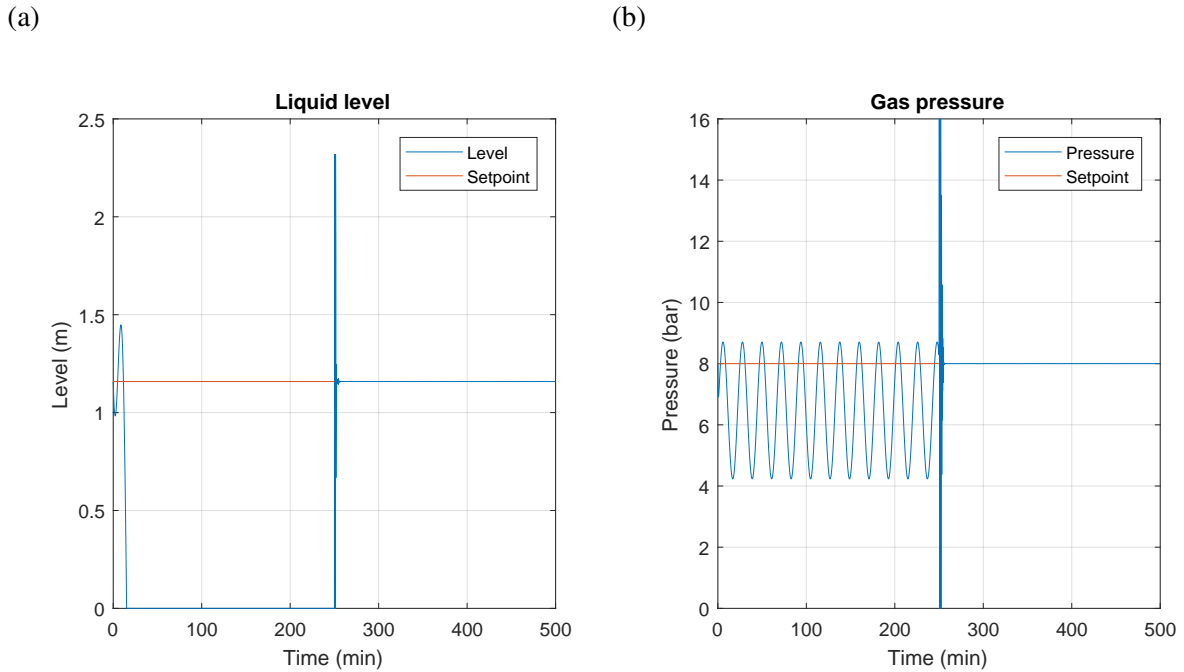
Figure 42 – Before and after turning the controller on: (a) Valves, (b) Outlet flow.
(a)   (b)
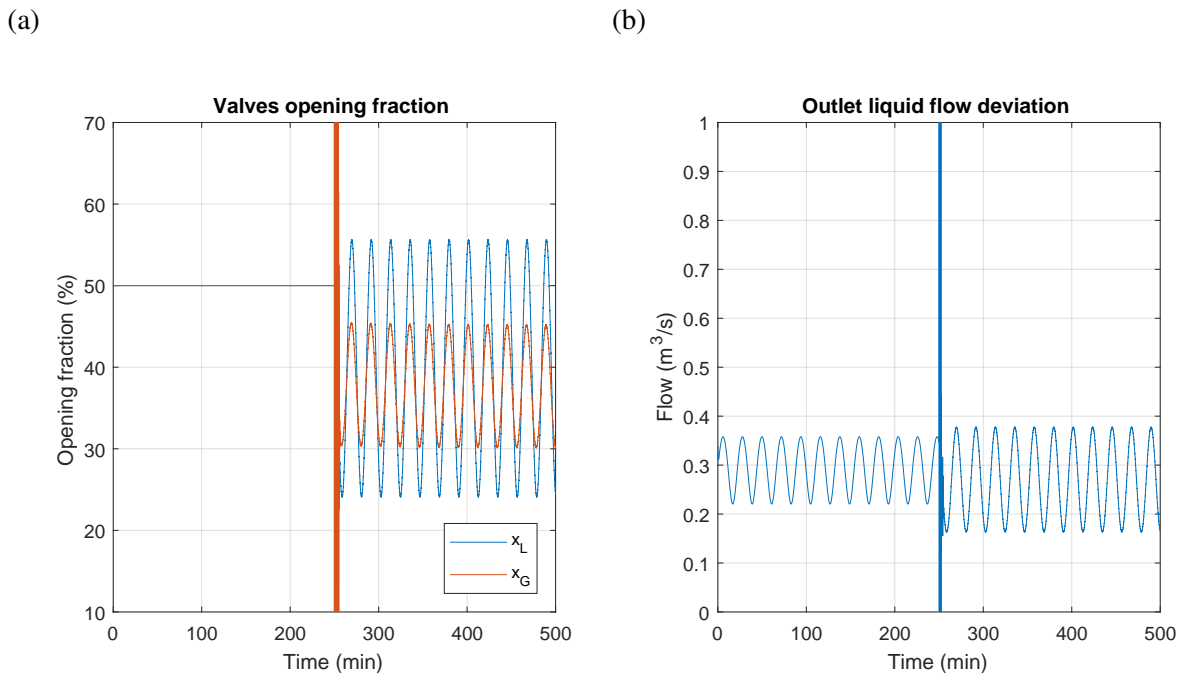
Next, the system is in its steady state conditions and there is a step change in the setpoints from $G_{in} = 0.16 \ m^3/s$ and $L_{in} = 0.08 \ m^3/s$ to $G_{in} = 0.28 \ m^3/s$ and $L_{in} = 0.14 \ m^3/s$ in minute 250. Figures 43 and 44 show how the system behaves to these changes.

Figure 43 – Step on steady state conditions: (a) Liquid level, (b) Gas pressure.
(a)   (b)
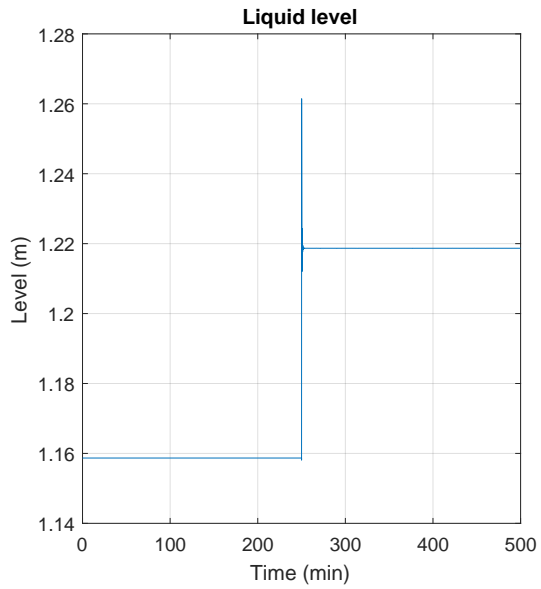
Figure 44 – Step on steady state conditions: (a) Valves, (b) Outlet flow.
(a)   (b)

5 CONCLUSION

Two PID controllers are optimized via a Genetic Algorithm meta-heuristic approach. The goal is to minimize variations in liquid level, gas pressure, valve opening fraction and outlet liquid flow in a horizontal biphasic separator tank. The algorithm excelled in controlling liquid level and g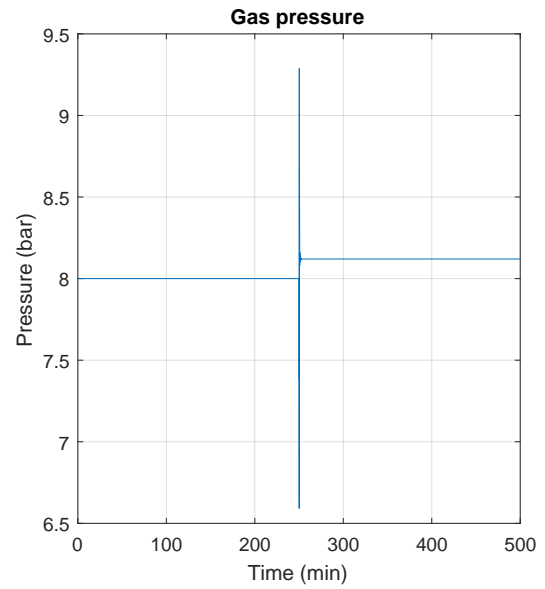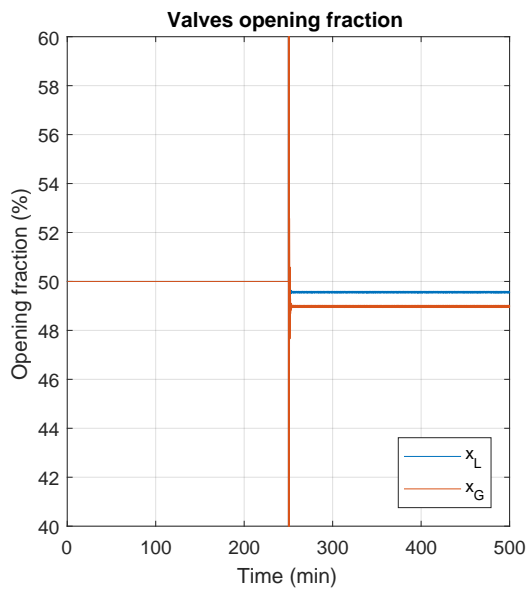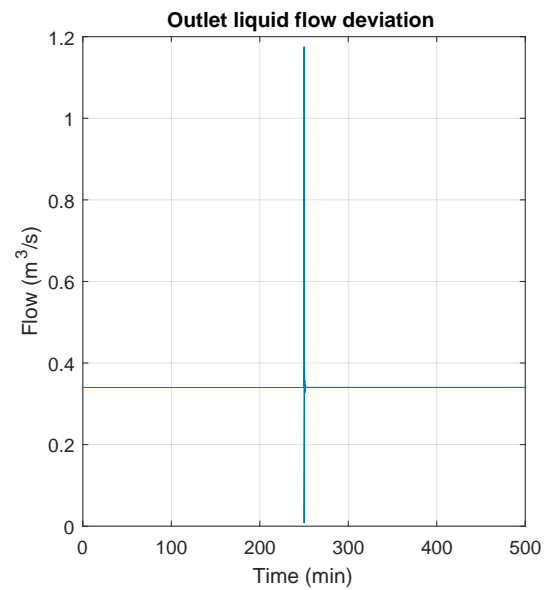as pressure in few iterations, keeping them close to the set point with almost no disturbance at all. Valves opening fractions presented good operation range, with a maximum amplitude of around 30%. Outlet liquid flow control had the worst performance, with percentual variations ranging from roughly 100% to 375%.

Even though the liquid valve opening fraction reached a minimum of 25%, that is, exceeding the ideal range presented by Poligon Válvulas Industriais (2014) in 5%, its operation range is still acceptable. The operational range from Poligon Válvulas Industriais (2014) has a 50% amplitude, where the maximum amplitude reached by the optimization is 30%.

Outlet liquid flow variation is explained by liquid level and gas pressure stability. In order to keep them close to the set point, the valves should be opening and closing accordingly to the inlet flow, thus mimicking the intermittent behavior. The optimization is not able to damp this response, probably because the feedback loop is minimizing liquid level and gas pressure and not the outlet flow. This would also explain why these variables were kept roughly constant. Since the control loops are around level and pressure, tendency is that they will converge to the set point, faster or slower. Controlling outlet liquid flow via GA can not "fight" liquid level and gas pressure control via PID since this is a "first instance error minimizer".

When compared to a previous study from Kindermann (2017), the GA-PID arrangement performs better then the PSO-P in controlling liquid level and gas pressure, while outlet liquid flow and valves opening fractions are roughly the same. This is probably due to the change from a proportional controller to a PID, since the PSO algorithm is likely to perform better than the GA in finding the global optimum (ARORA, 2004; FLOREANO; MATTIUSSI, 2008).

The calculated parameters can control the system well as it can be seen from the experiments when the controller is turned on after 250 minutes of slug flow without the control, and when there is a step change to the system setpoints.

Future works may cover the effect of a PID loop over liquid and gas outlet flows instead of liquid level and gas pressure to minimize outlet flow variation, three-phase gravity separation tank simulation, series of separator tanks with pressure steps between them, a more robust slug flow simulation instead of trigonometric functions, well-separator coupling and reservoir-well-separator coupling.

BIBLIOGRAPHY

AHMADI, M. A. et al. Evolving artificial neural network and imperialist competitive algorithm for prediction oil flow rate of the reservoir. **Applied Soft Computing**, Elsevier, v. 13, n. 2, p. 1085–1098, 2013.

ARORA, J. **Introduction to optimum design**. Iowa City: Academic Press, 2004.

BAI, Q.; BAI, Y. **Sistemas Marítimos de Produção de Petróleo: Processos, Tecnologias e Equipamentos Offshore**. Rio de Janeiro: Elsevier Brasil, 2016.

BIANCHI, L. et al. A survey on metaheuristics for stochastic combinatorial optimization. **Natural Computing: an international journal**, p. 239–287, 2009.

BOYCE, W. E.; DIPRIMA, R. C. **Equações Diferenciais Elementares e Problemas de Valores de Contorno**. Teresópolis: LTC, 2004. v. 8.

CAMARGO, E. et al. Optimization model based on genetic algorithms for oil wells. In: WORLD SCIENTIFIC AND ENGINEERING ACADEMY AND SOCIETY (WSEAS). **Proceedings of the 9th WSEAS international conference on computational intelligence, man-machine systems and cybernetics**. [S.l.], 2010. p. 131–139.

CAMPOS, M. et al. Advanced anti-slug control for offshore production plants. **IFAC-PapersOnLine**, Elsevier, v. 48, n. 6, p. 83–88, 2015.

FLOREANO, D.; MATTIUSSI, C. **Bio-Inspired Artificial Intelligence**: Theories, methods, and technologies. London: The MIT Press, 2008. v. 1.

GHAEDI, M.; EBRAHIMI, A. N.; PISHVAIE, M. R. Application of genetic algorithm for optimization of separator pressures in multistage production units. **Chemical Engineering Communications**, Taylor & Francis, v. 201, n. 7, p. 926–938, 2014.

GODHAVN, J.-M.; FARD, M. P.; FUCHS, P. H. New slug control strategies, tuning rules and experimental results. **Journal of Process Control**, 2004.

GÜYAGÜLER, B. et al. Optimization of well placement in a gulf of mexico waterflooding project. **SPE Reservoir Evaluation & Engineering**, Society of Petroleum Engineers, v. 5, n. 03, p. 229–236, 2002.

KINDERMANN, E. **Otimização Meta-Heurística de um Separador Bifásico com Parâmetros Geométricos e de Controle Proporcional**. 2017. Term paper.

MATLAB. **version 7.9.0 (R2009b)**. Natick, Massachusetts: The MathWorks Inc., 2009.

NUNES, G. C.; MEDEIROS, J. L. de; ARAUJO, O. de Q. F. **Modelagem e Controle na Produção de Petróleo**. São Paulo: Blucher, 2010. v. 1.

Poligon Válvulas Industriais. **A importância de rangeabilidade em válvulas de controle**. São Paulo: Poligon Válvulas Industriais, 2014. Boletim Comparativo de Rangeabilidade das Válvulas de Controle VEC® e Globo.

ROMERO, C.; CARTER, J. Using genetic algorithms for reservoir characterisation. **Journal of Petroleum Science and Engineering**, Elsevier, v. 31, n. 2, p. 113–123, 2001.

SEBORG, D. E. et al. **Process Dynamics and Control**. Hoboken: John Wiley & Sons, Inc., 2011. v. 1.

SILVA, A. L. F. da et al. **Processamento Primário de Petróleo**. Rio de Janeiro: Petrobras, 2007. v. 1.

STASIAK, M. E.; PAGANO, D. J.; PLUCENIO, A. A new discrete slug-flow controller for production pipeline risers. **IFAC Proceedings Volumes**, Elsevier, v. 45, n. 8, p. 122–127, 2012.

STEWART, J. **Cálculo**. São Paulo: Pioneira Thomson Learning, 2006. v. 1.

STEWART, J. **Cálculo**. São Paulo: Pioneira Thomson Learning, 2007. v. 2.

SWINDELL, R. Hidden integrity threat looms in subsea pipework vibrations. **Offshore Magazine**, Tulsa, v. 71, 2011.

YANG, X.-S. **Nature-inspired metaheuristic algorithms**. Frome: Luniver press, 2010.

Annex

ANNEX A – EXAMPLES

Example 1

The Laplace Transform of $f(t) = e^{at}$ is

$$\begin{aligned}
\mathscr{L}\{e^{at}\} &= \int_0^\infty e^{-st} e^{at} dt \\
&= \int_0^\infty e^{-(s-a)t} dt \\
&= \frac{1}{s-a}, \ \ s > a.
\end{aligned} \tag{A.1}$$

Example 2

Let $f(t)$ be a function which derivative is $f'(t)$. The Laplace Transform of the derivative is

$$\mathscr{L}\{f'(t)\} = \int_0^\infty e^{-st} f'(t) dt \tag{A.2}$$

This integral is solved by parts, being $dv = f'(t)dt$ and $u = e^{-st}$, resulting in $v = f(t)$ and $du = -se^{-st}dt$:

$$\int u\,dv = vu - \int v\,du$$

$$\int_0^\infty e^{-st} f'(t) dt = [e^{-st} f(t)]_0^\infty + s \int_0^\infty e^{-st} f(t) dt. \tag{A.3}$$

Applying the limits in the first term on the right hand side yields $-f(0)$. Paying attention to the second term, it is possible to see that it is but the Laplace Transform definition itself from Equation 2.7, multiplied by s. Therefore, the Laplace Transform of the derivative of a function is:

$$\mathscr{L}\{f'(t)\} = s\mathscr{L}\{f(t)\} - f(0). \tag{A.4}$$

The Laplace Transform of the second derivative of a function, $f''(t)$:

$$\mathscr{L}\{f''(t)\} = \int_0^\infty e^{-st} f''(t) dt.$$

Solving this integral by parts in such a way that $dv = f''(t)dt$ and $u = e^{-st}$, resulting $v = f'(t)$ and $du = -se^{-st}dt$:

$$\int_0^\infty e^{-st} f''(t) dt = [e^{-st} f'(t)]_0^\infty + s \int_0^\infty e^{-st} f(t)' dt.$$

$$\mathscr{L}\{f''(t)\} = s\mathscr{L}\{f'(t)\} - f'(0).$$

Substituting this result in Equation A.4 yields

$$\mathscr{L}\{f''(t)\} = s^2 \mathscr{L}\{f(t)\} - sf(0) - f'(0). \tag{A.5}$$

In fact this pattern repeats itself for any derivative of $f(t)$, allowing us to write

$$\mathscr{L}\{f^{(n)}(t)\} = s^n \mathscr{L}\{f(t)\} - s^{n-1} f(0) - \cdots - sf^{(n-2)}(0) - f^{(n-1)}(0). \tag{A.6}$$

Example 3

Let $S(t)$ be a step function,

$$S(t) = \begin{cases} 0, & t < t_0 \\ 1, & t \geq t_0. \end{cases} \tag{A.7}$$

In order to apply the Laplace Transform in this function, it must be divided in two intervals: from 0 to t_0 and from t_0 to ∞,

$$\mathscr{L}\{S(t)\} = \int_0^{t_0} e^{-st} S(t < t_0) dt + \int_{t_0}^\infty e^{-st} S(t \geq t_0) dt. \tag{A.8}$$

Since $S(t < t_0) = 0$ by definition, it is only needed to solve the second integral, where $S(t \geq t_0) = 1$,

$$\mathscr{L}\{S(t)\} = \int_{t_0}^\infty e^{-st} dt = \frac{e^{-st_0}}{s}. \tag{A.9}$$

Example 4

The tank presented in Figure 1 is described by Equation 2.3,

$$A\frac{dh}{dt} = q_i - \frac{1}{R_v}h. \tag{2.3}$$

Suppose the tank is initially empty and there is no flow occuring, $h(0) = 0$ and $q_i(0) = 0$, when a flow Q starts to fill the tank. This means $q_i(t)$ is a step function $S(t)$ with $t_0 = 0$, multiplied by Q. Applying the Laplace Transform:

$$\mathscr{L}\left\{A\frac{dh}{dt}\right\} = \mathscr{L}\left\{QS(t) - \frac{1}{R_v}h\right\}.$$

Due to the linearity property of the operation, the previous expression can be written as

$$A\mathscr{L}\left\{\frac{dh}{dt}\right\} = Q\mathscr{L}\{S(t)\} - \frac{1}{R_v}\mathscr{L}\{h\}.$$

From Table B.1, formulas 2 and 13 are applied to the previous equation, being $f(t) = h(t)$ and $F(s) = H(s)$,

$$A[sH(s) - h(0)] = Q\frac{1}{s} - \frac{1}{R_v}H(s).$$

Since $h(0) = 0$, it is possible to solve this equation for $H(s)$ as

$$H(s) = QR_v\frac{1}{s(AR_vs + 1)}. \tag{A.10}$$

It is possible now to apply the Inverse Laplace Transform to find $h(t)$. From Table B.1, int can be seen that $H(s)$ equals the second column of formula 7, multiplied by QR_v and being $\tau = AR_v$,

$$h(t) = QR_v(1 - e^{-t/AR_v}). \tag{A.11}$$

This result can be verified by being differentiated in respect to time and multiplied by A, which should be equal to $q_i - h/R_v$, as shown by Equation 2.3.

Exemple 5

For θ close to 0, the function sen θ can be approximated by

$$\text{sen } \theta = \sum_{n=0}^{\infty} \frac{f^{(n)}(0)}{n!} \theta^n. \tag{A.12}$$

Also, derivatives of sen θ are cyclical after the fourth differentiation:

$$\begin{cases} \frac{d\text{sen } \theta}{d\theta} = \cos \theta; \\ \frac{d^2\text{sen } \theta}{d\theta^2} = \frac{d\cos \theta}{d\theta} = -\text{sen } \theta; \\ \frac{d^3\text{sen } \theta}{d\theta^3} = \frac{d(-\text{sen } \theta)}{d\theta} = -\cos \theta; \\ \frac{d^4\text{sen } \theta}{d\theta^4} = \frac{d(-\cos \theta)}{d\theta} = \text{sen } \theta. \end{cases}$$

Knowing that sen $0 = 0$ and $\cos 0 = 1$, the first terms of A.12 can be calculated as

$$\text{sen } \theta = \frac{\text{sen } 0}{0!} + \frac{\cos 0}{1!}\theta - \frac{\text{sen } 0}{2!}\theta^2 - \frac{\cos 0}{3!}\theta^3 + \frac{\text{sen } 0}{4!}\theta^4 + \frac{\cos 0}{5!}\theta^5 + \cdots$$

$$\text{sen } \theta = \theta - \frac{\theta^3}{3!} + \frac{\theta^5}{5!} - \frac{\theta^7}{7!} + \cdots$$

$$\text{sen } \theta = \sum_{n=1}^{\infty} (-1)^{(n-1)} \frac{\theta^{(2n-1)}}{(2n-1)!}. \tag{A.13}$$

This summation will approximate the function by an n-th degree polynomial. Approximating sen (0.1) by a Maclaurin Series truncated in the second term yields

$$\text{sen } (0.1) = 0.099833416... \quad \text{(Real Value)}$$

$$\text{sen } (0.1) \approx 0.1 - \frac{0.1^3}{3!} = 0.099833333... \quad \text{(Approximated Value)}$$

The divergence occurs in the seventh decimal place with a percentual error of $8.34 \times 10^{-5}\%$.

ANNEX B – LAPLACE TRANSFORMS

Table B.1 – Laplace Transforms

$f(t)$	$\mathcal{L}\{f(t)\} = F(s)$
1. $\delta(t)$ (unit impulse)	1
2. $S(t)$ (unit step, $t_0 = 0$)	$\dfrac{1}{s}$
3. t (ramp)	$\dfrac{1}{s^2}$
4. $\dfrac{1}{\tau}e^{-t/\tau}$	$\dfrac{1}{\tau s+1}$
5. $\dfrac{1}{\tau_1-\tau_2}(e^{-t/\tau_1} - e^{-t/\tau_2})$	$\dfrac{1}{(\tau_1 s+1)(\tau_2 s+1)}$
6. $\dfrac{1}{\tau_1}\dfrac{\tau_1-\tau_3}{\tau_1-\tau_2}e^{-t/\tau_1} + \dfrac{1}{\tau_2}\dfrac{\tau_2-\tau_3}{\tau_2-\tau_1}e^{-t/\tau_2}$	$\dfrac{\tau_3 s+1}{(\tau_1 s+1)(\tau_2 s+1)}$
7. $1 - e^{-t/\tau}$	$\dfrac{1}{s(\tau s+1)}$
8. $\operatorname{sen} \omega t$	$\dfrac{\omega}{s^2+\omega^2}$
9. $\cos \omega t$	$\dfrac{s}{s^2+\omega^2}$
10. $\operatorname{sen}(\omega t + \phi)$	$\dfrac{\omega \cos \phi + s \operatorname{sen} \phi}{s^2+\omega^2}$
11. $e^{-bt}\operatorname{sen} \omega t$	$\dfrac{\omega}{(s+b)^2+\omega^2}$
12. $e^{-bt}\cos \omega t$	$\dfrac{s+b}{(s+b)^2+\omega^2}$
13. $f^{(n)}(t)$	$s^n F(s) - s^{n-1}f(0) - \cdots - sf^{(n-2)}(0) - f^{(n-1)}(0)$
14. $f(t - t_0)S(t - t_0)$	$e^{-t_0 s}F(s)$

Source: adapted from SEBORG et al. (2011).